Danko Taboroši, Kazuomi Hirakawa, and Takanobu Sawagaki - Carbonate precipitation along a microclimatic gradient in a Thailand cave - Continuum of calcareous tufa and speleothems. *Journal of Cave and Karst Studies*, v. 67, no. 1, p. 69-87.

CARBONATE PRECIPITATION ALONG A MICROCLIMATIC GRADIENT IN A THAILAND CAVE – CONTINUUM OF CALCAREOUS TUFA AND SPELEOTHEMS

DANKO TABOROŠI
Laboratory of Geoecology, Graduate School of Environmental Earth Science, Hokkaido University, N-10 W-5, Sapporo, JAPAN 060-0810
taborosi@gmail.com
KAZUOMI HIRAKAWA
Laboratory of Geoecology, Graduate School of Environmental Earth Science, Hokkaido University, N-10 W-5, Sapporo, JAPAN 060-0810
hkazu@ees.hokudai.ac.jp
TAKANOBU SAWAGAKI
Laboratory of Geoecology, Graduate School of Environmental Earth Science, Hokkaido University, N-10 W-5, Sapporo, JAPAN 060-0810
sawagaki@ees.hokudai.ac.jp

Variations in the local microclimate can profoundly affect vadose carbonate precipitation. This may be negligible deep inside caves, but is intense in climatically less stable environments, such as cave entrances and twilight zones. In such settings, microclimate can exert primary control on the characteristics of actively forming stalactites, far outweighing the other factors, notably dripwater properties.

Based on temperature, humidity, and light intensity monitoring of a cave in southern Thailand and analyses of associated cave deposits, we have seen that microclimatic (and ensuing biologic) gradients that exist between the cave entrance and cave interior are closely reflected by the morphology and petrology of actively forming stalactites. Spanning the cave's microclimatically most variable and most stable parts, these stalactites comprise uninterrupted morphologic and petrologic series, ranging from extremely porous and largely biogenic stalactitic accretions of calcareous tufa growing around the dripline (and even outside the cave) to the dense coarsely crystalline stalactites (speleothems) in the cave interior. This rarely observed continuum between tufas and speleothems indicates that the boundary between the two is hardly distinct (or justified) and any observed differences can be simply a result of different microclimatic regimes of their depositional settings.

In this paper we will demonstrate that the local environment can exert primary control on the characteristics of actively forming stalactites, producing a far greater morphologic and petrologic range than other factors, specifically dripwater properties, are known to bring about. We will show that the end members of this range correspond to calcareous tufa and speleothem travertine, and that the two are not necessarily distinct types of sediments but parts of a continuum of genetically allied carbonate fabrics mediated by environmental factors.

There are two variables that control the abiotic precipitation of carbonate speleothems, as karst waters emerge from bedrock and enter karst cavities (Atkinson & Smith 1976, Dreybrodt 1988). These are the properties of 1) water dripping into a cave, and of 2) environment within a cave. Both directly influence carbonate precipitation and, combined, they account for most of the morphologic, mineralogic, and petrologic properties of speleothems. While the links between volumes, rates and geochemistry of water with the crystal habit and structure of speleothems (e.g., Given & Wilkinson 1985, Gonzales *et al*. 1992, Frisia *et al*. 2000, 2002) and other freshwater carbonates (e.g., Emeis *et al*. 1987, Chafetz *et al*. 1991) have been extensively studied, the influence of local environmental factors has remained largely unaddressed since early inquiries established that its importance is secondary to water properties (Gams 1968). Nonetheless, environmental factors, microclimate in particular, can have significant impact on the formation of speleothems. Microclimatic parameters, especially temperature and humidity, are known to affect the deposition of speleothems (e.g., Harmon *et al*. 1983, Railsback *et al*. 1994, Borsato *et al*. 2000) and genetically allied tufas (e.g., Pedley *et al*. 1996). This should be clear even intuitively, from the simple observation that stalactites regularly grow in the humid atmosphere of caves, but are normally not expected to form at the land surface where their growth is limited by evaporative effects (Hill & Forti 1997).

However, any study attempting to relate particular microclimatic conditions with stalactite properties faces unique design problems: research within a single cave is nearly impracticable because of minuscule spatial variability of microclimatic parameters (e.g., Buecher 1999), whereas comparative research on several caves is precluded by the existence of too many added variables, which make any impact of microclimate on carbonate fabrics difficult to isolate and assess. Opportunely, cave entrances can show significant spatial variability in the microclimate, while keeping the other numerous parameters essentially even. This is perhaps not so obvious in classical karst regions, where the small entrances and infinitesimal width-to-length ratios of fluviokarst caves

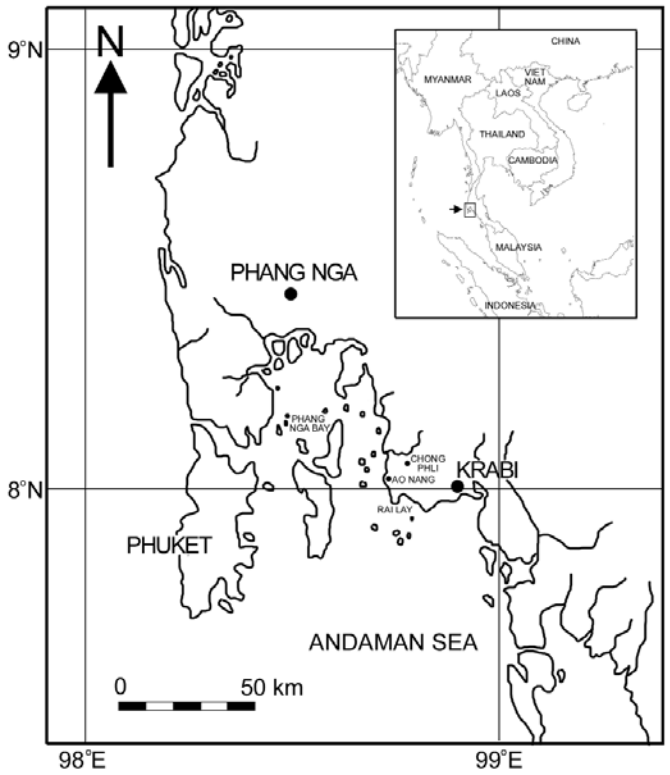

Figure 1. Location map of Krabi area in southern Thailand, with locales mentioned in text.

(Ford & Ewers 1978, Bögli 1980) combined with the stark climatic contrasts between the epigean and spelean realms (Cropley 1965) result in limited air circulation, sharp microclimatic clines at the entrances, and little variation elsewhere. In tropical areas, however, 1) cave entrances are often enormous, formed by collapse rather than speleogenesis per se; 2) certain cave types exhibit widths greater than their lengths (Mylroie & Carew 1995); and 3) generally high and stable outside humidity and temperature levels do not radically differ from cave interiors. Actually, in the humid tropics, stalactites can be prolific even outside of caves (Sweeting 1973, Longman & Brownlee 1980, Jennings 1985, Taboroši *et al*. 2003a, 2003b), indicating that microclimatic conditions necessary for their growth can be found in parts of the epigean environment, as well. All of these factors contribute to less "dramatic" transitions between the epigean and spelean environments in the tropics as opposed to temperate areas, thereby producing more gentle microclimatic gradients over greater distances in the tropical caves. Indeed, in some tropical caves with large entrances, the transitional ("twilight") zones between the land surface and cave interiors are so broad that they exhibit distinct microclimates of their own, ceasing to be mere interfaces between epigean and spelean realms. Enclosed enough to sustain abundant stalactite growth, yet open enough to exhibit considerable light penetration and marked diurnal fluctuations in temperature and humidity, these large entrances of tropical caves present nearly ideal natural laboratories for evaluating environmental impact on the morphology and fabrics of vadose carbonate precipitates.

In our initial assessment of links between microclimatic parameters and the properties of stalactites, based on observations from Guam, Mariana Islands, we have demonstrated that the two are indeed closely related (Taboroši & Hirakawa 2003). The present study, carried out in a single cave in Krabi Province, Thailand, builds on those foundations and refines the original work by applying improved methodology and demonstrating a wider geographic relevance. Following a thorough examination of spatial and temporal variations in temperature, humidity, evaporation rates, and light levels experienced by different parts of the cave, we related that environmental data to the petrologic properties of actively forming stalactitic deposits. We found that the deposits range from highly porous and largely biogenic accretions of calcareous tufa (shaped convincingly like stalactites) growing at the entrance to the dense coarsely crystalline stalactites in the cave's interior. These deposits display a wide range of distinct fabrics forming an uninterrupted morphologic and petrologic series, as they span the microclimatically most variable and most stable parts of the cave. Because certain stalactite morphologies and fabrics appear to form under highly specific environmental conditions, these observations promise to be a valuable tool in paleoenvironmental interpretation.

STUDY AREA

The study was carried out in Krabi Province, southern Thailand (Fig. 1). The area has been described as "some of the most geologically interesting and scenically stunning landscape" in the world (Wasseman 1984) and is characterized by steep cliffs and immense karst towers developed in massive Permian limestone (Waterhouse 1981). The limestone towers, belonging to the vertical-walled turmkarst and cone-shaped kegelkarst types, emerge from shallow waters of Phang Nga Bay or mangrove swamps along the coast, and from Quaternary alluvial plains in inland areas (Harper 1999). The local climate is tropical monsoonal, and most of the average annual rainfall of 2379 mm falls from May to October. The wettest month is usually September, and the driest is February, with 361 mm and 25 mm of rain respectively. The mean daily temperature is 28.1°C (min. 24.0°C; max. 31.3°C), while the average relative humidity ranges from 68% in February to 81% in October (Sarigabutr *et al*. 1982).

The studied cave (Fig. 2) is located at the base of an isolated 40-m-tall vertical-walled tower in the village of Chong Phli, 15 km from Krabi town and 5 km northeast of Ao Nang beach. The cave, named Pop Kan Mai, was discovered during an informal field survey of the area. Although it is well known to the local people of the village, it seems to be rarely visited and does not appear to be referenced in Thai cave compendia (e.g., Dunkley 1994, 1995). The cave's entrance area is defined by overhanging rock at the base of the tower, and is thoroughly

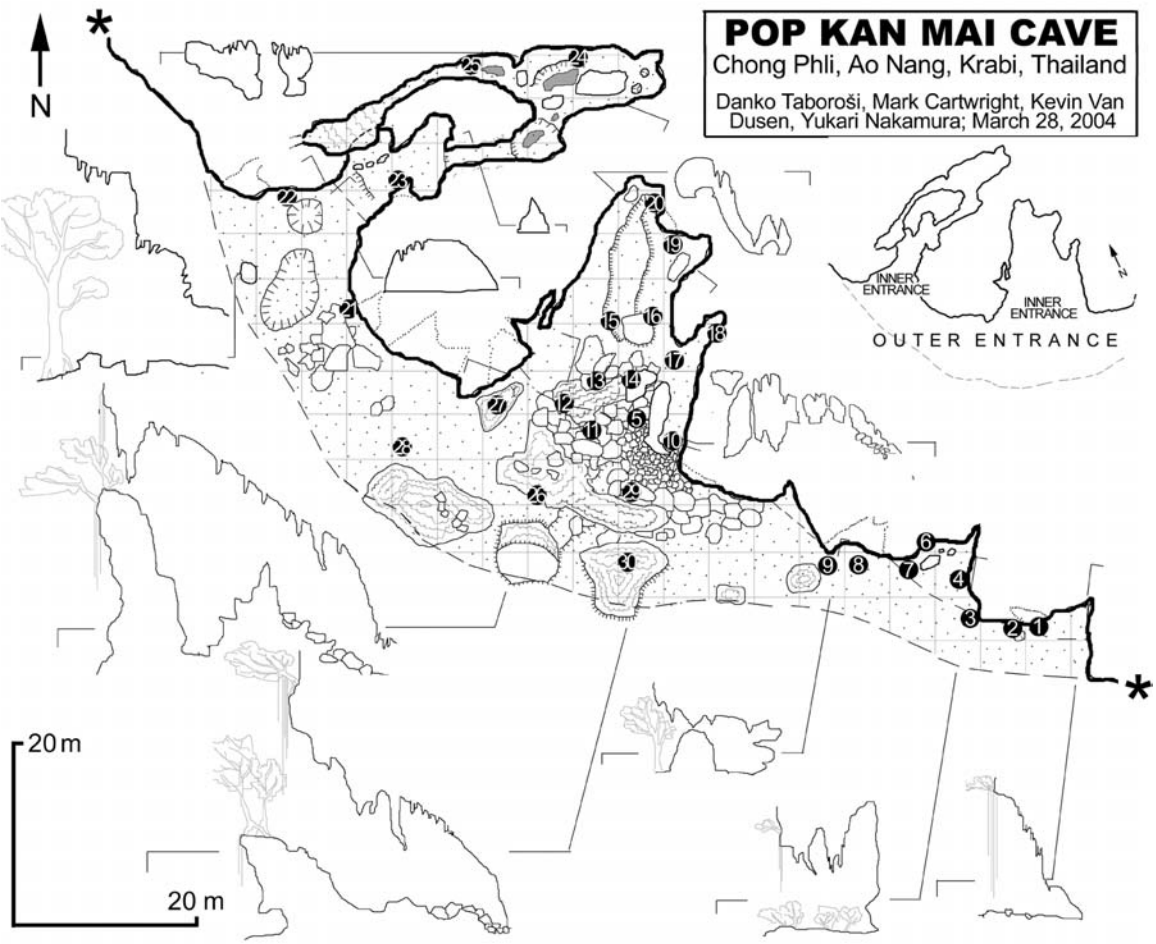

Figure 2. Plan and selected profiles of Pop Kan Mai Cave. Numbered black dots indicate stalactite sample locations and sample ID numbers. Grid cells are 5 m x 5 m. Dashed line represents the dripline and the two asterisks (*) indicate continuing karst tower cliff line. Inset shows the extent of what we termed "outer entrance" and "inner entrances."

concealed behind a thick, curtain-like canopy of vines and roots of trees growing at the top of the cliff. Following the perimeter of the tower, the undercut area is over 100 m wide and up to 20 m tall at the dripline. This spacious zone, designated as "outer entrance", accounts for more than half of the total area of the cave and is covered by colluvium and soil, piles of collapse blocks and large boulders, and inactive remnants of flowstone banks. Within 5–15 m inward from the dripline, the slanting roof meets the inner vertical wall of the undercut, forming a shelter cave along most of the width of the outer entrance, except in two places where inner entrances lead to separate cavities. The larger of the two inner entrances, 20 m wide and up to 3 m tall, is to the southeast and is partly blocked by collapse. It leads to a single down-sloping chamber, that branches off to several minor passages, which promptly pinch off, evoking the morphology of flank margin caves (Mylroie & Carew 1990). The other, smaller inner entrance is located some 20 m to the northwest, and is 8 m wide and 3.5 m tall. This cavity exhibits markedly different morphology from the previous, and consists of a narrow, mostly horizontal linear passage that extends 25 m northeast to a small chamber, from where it meanders and continues 25 m in the opposite direction, until it becomes to tight to follow. This passage is inhabited by a bat colony in excess of 100 individuals.

METHODOLOGY

The project was comprised of three components: 1) surveying of the cave and preparation for subsequent work; 2) monitoring and assessment of microclimate; and 3) sampling and analyses of local stalactites. Fieldwork was carried from March 12 until April 17, 2004.

The cave was surveyed applying standard National Speleological Society techniques (Dasher 1994), using a compass, clinometer, and metric tape. Following the drafting of the map, a 5-m grid was superimposed on it (Fig. 2), each grid square was numbered, and corresponding markers were placed in the field. This was done to improve the spatial accuracy of subsequent work in microclimate measurements and stalactite sampling.

Microclimate was evaluated by data loggers, evaporation pans, and periodic spot measurements. Data loggers were used to monitor temperature, humidity, and light intensity. The same

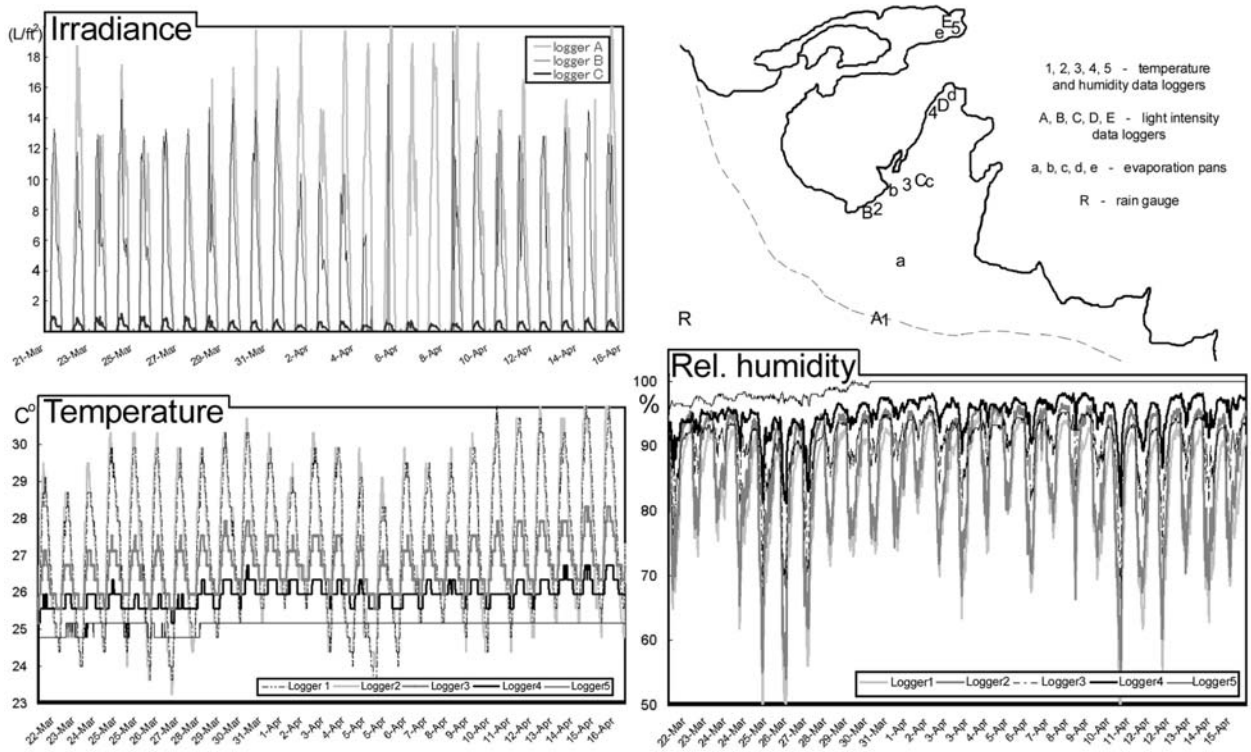

Figure 3. Data recorded by microclimate sensors in Pop Kan Mai Cave. The simplified plan shows positions of the data loggers. Temperature/ humidity sensors, light intensity sensors, and evaporation pans are denoted by numbers, capital letters, and lower-case letters, respectively. Note that mostly straight horizontal temperature and humidity lines correspond to conditions at the back of the cave (logger 5), and that the minor oscillations in humidity seemingly stabilize at 100%, as a consequence of the sensor's worsened performance in a high humidity environment. Light intensity values obtained by the innermost light intensity sensors (D and E) are constantly zero and are not shown in the graph.

parameters were checked by occasional spot readings, during which time photosynthetic photon flux and presence of air currents were also assessed. Temperature and humidity were monitored using Onset Hobo® H8 Pro data loggers, whose sensors record temperature between –30 and +50°C (with an accuracy of ±0.2°C and a resolution of 0.02°C) and humidity from 0% to 100% on a relative scale (with an accuracy of up to ±4% in condensing environments, such as cave interiors). The specified accuracy levels were deemed adequate for the purposes of our research, considering that the goal was a comparative assessment of microclimatic conditions rather than obtaining absolute values. Light intensity was measured by Hobo® LI data loggers, whose specifications indicate a wide spectral response and a range from less than 0.01 lm/ft² (0.11 lx) to over 10,000 lm/ft² (1.08 x 10^5 lx) or full sunlight. To avoid condensation damage to LI sensors, they were placed in clear quartz glass jars with silica desiccants. The data loggers were attached to cave ceilings or walls, roughly delineating a horizontal transect from the entrance to cave interior (Fig. 3). Loggers in the cave entrance were carefully placed in order to avoid exposure to direct sunlight, which would cause exaggerated readings. Loggers were set to collect temperature and relative humidity measurements every 15 minutes and light intensity readings every 60 minutes, during the period from March 21, 2004 until April 16, 2004. In addition, five plastic pans (surface area 104 cm²) with drip shields were filled with exactly 350 mL of water by using volumetric flasks and placed throughout the cave (Fig. 3). The volume of water necessary to restore the original volume was measured after 28 days, and evaporation rates were calculated in mL/m²/day. Securing the evaporation pans and data loggers was particularly challenging and we had to use strong wire and mesh casings to prevent macaque monkeys and tree shrews, which frequent the site, from tampering with them. Several days worth of data were lost from one of our LI loggers due to animal interference, and the plastic casing of one H8 Pro data logger had deep gnaw marks left by a tree shrew.

Besides long term monitoring, we took several series of spot measurements, each as contemporaneously as possible, at dozens of points throughout the cave, at all stalactite sample sites, and along a number of horizontal transects. These were used to validate data logged by sensors and obtain additional data for improved understanding and mapping of the cave's microclimate. Temperature and humidity were measured by a hand-held thermometer/psychrometer and irradiance levels were checked by a light meter. Airflow was gauged by a digi-

tal anemometer with a resolution of 0.2 m/s. In order to assess the light energy at wavelengths available to plant and microphyte growth, we have estimated photosynthetically active radiation (PAR) by a Spectrum Technologies quantum meter and obtained relative measurements by comparison with unobstructed sky. Finally, a tipping bucket rain gauge was installed near the cave, but the area experienced only a single day of significant rainfall during the fieldwork period.

Thirty stalactites to be sampled were chosen by randomly selecting thirty 5 x 5 m squares in the prepared grid and picking one actively dripping specimen growing within each square. Nine squares lacked stalactitic deposits, so samples were taken from other areas by judgment and convenience (all sample locations are indicated on Fig. 2). Actively dripping specimens were chosen in order to ensure that only contemporary, diagenetically-unaltered deposits growing in equilibrium with the present microclimate are considered. Drip rates were measured on several days and found to vary dramatically with time. Most of the specimens actually ceased to drip by the end of the fieldwork period, due to the lack of rainfall. Prior to the collection of stalactites, each specimen was photodocumented, measured and thoroughly examined in situ (Table 1). At the end of the fieldwork period, samples were removed by hammer and chisel and no preservation methods were used to treat them. They were allowed to dry at room temperature in the lab for several weeks prior to analyses. Following cutting, and macroscopic and binocular microscope examination, the samples were studied through conventional transmitted-light microscopy of resin-impregnated petrographic thin sections (one transverse and one longitudinal per specimen). Additionally, small fragments (two or three per specimen) were glued to aluminum stubs, sputter-coated with platinum and observed with a Hitachi S-3000H Scanning Electron Microscope (SEM), under operating conditions at 20 kV and 60 µA. Mineralogy was ascertained by X-ray diffraction (XRD) analyses on a Bruker AXS MX-Labo powder diffractometer.

RESULTS

CAVE MICROCLIMATE

We describe the microclimatic environment of the cave in terms of four factors: temperature, humidity, light availability, and airflow that can be expected to affect carbonate deposition. The first two are intrinsic parameters, which directly affect the chemistry of precipitation. Light levels have no immediate impact, but can indirectly affect the process by defining the local biologic environment. Airflow can physically influence stalactite formation.

TEMPERATURE, HUMIDITY AND EVAPORATION RATES

Microclimate of the studied cave is defined by cooler, more humid and stable conditions in the rear, and greater variability toward the entrance (Fig. 4). The temperature regime is characterized by 1) a distinct pattern of daily variations at the entrance; 2) a gradual buffering of daily temperature changes toward the interior of the cave, so that both minimum and maximum values experienced are progressively closer to the mean; and 3) a stable temperature in the farthest portions of the cave (Fig. 3). Therefore, although the temperatures throughout the cave are comparable in terms of mean values, with an average of 27.3° C in the outer entrance and 25.1° C in the cave's innermost part, they greatly differ over time. Maximum temperatures in outermost parts of the cave reached 31.5° C, while the temperature deeper inside the cave never exceeded 25.2° C. The daily temperature range is reduced by 8.3° C in the outer entrance and by 3.1° C in the inner entrance and dwindles to a virtually constant temperature further inside. Statistical analysis indicated that the variance in temperatures decreases from the entrance, with coefficients of variance ranging from 6.9° C in the outer entrance and approaching zero inside the cave (Table 2).

Relative humidity changes exhibit a similar pattern, except that there is a clear increase in mean values toward the cave's interior (Fig. 4). The overall situation is thus typified by 1) the greatest range and lowest relative humidity values at the entrance; 2) progressive increase of minimum and mean values toward the cave interior; and 3) nearly constant, ~100% levels deeper inside the cave (Fig. 3). In the outer entrance, the relative humidity shows an average of 83% and a coefficient of variance of 11, while in the inner entrance, the mean is 90% and a coefficient of variance is five (Table 2). The humidifying effect of the cave entrance is even more apparent from the minimum values, which were 19% apart. Finally, in the rear of the cave, the data indicate largely stable and highly humid conditions in excess of 95%. Accordingly, evaporation rates dramatically decrease toward the interior of the cave (Fig. 4). While the outermost evaporation pan indicated a daily loss of 714 mL/m², the one placed deepest inside the cave was evaporating 36 mL/m²/day. One significant observation is that maximum relative humidity values regularly reach levels above 95% even in the cave's outermost entrance area (Table 2), and indeed, outside the cave as well. This indicates that high humidity characteristic of caves temporarily occurs at the land surface, and is surely one of the factors enabling the prolific growth of stalactites in cave entrances and even on limestone scarps in the tropics.

LIGHT LEVELS AND AIRFLOW

Light intensity levels, obviously, diminish toward the cave interior. Daylight penetration into caves declines exponentially (Pentecost & Zhaohui 2001) or shows sudden drops caused by passage configuration. Accordingly, most of the study cave's larger chamber to the southeast is penetrated by at least some daylight, whereas much of the narrow and winding linear passage is in complete darkness. The outermost parts of the cave, at the dripline, are best illuminated but rarely experience levels greater than a quarter of full daylight (Fig. 4). This is due to effective shading by the vegetation growing on the cliff face. Uneven distribution of this canopy and geometry of the

Table 1. Physical description and other characteristics of sampled stalactites.

Physical description		Position		~Size		Deflection		Exterior surface		Drips[f]		
#	[all samples are stalactitic]	D[a] (m)	H[b] (m)	L[c] (cm)	C[d] (cm)	Angle (deg)	Direc. note[e]	Texture	Visible plants & animals	4/9/04 (mL/day)	Tem. (°C)	RH (%)
3	Crooked, partly attached to wall	3	2	90	42	<10°	W-NW	velvety organic coating	algae, fungus, spiderweb	<1	32	72
2	Massive, bumpy base with 3 stalactites	3	3	165	180	variable <30°	N	bumpy, rough	roots, algae, mud waspi	<1	32.2	74
30	Irregular, enlarged pendant-like tip	3	~15	20	20	variable<10°	S-SW	rough, earthy	algal coating	n/a	32.2	73
4	Slightly arched, bumpy, with 2 tips	3	2.5	90	45	<10°	N	bumpy, rough	algal coating at the tip	2	32.1	73
1	Step-like, projecting out of the wall	4	3	36	54	variable 45-75°	S	smooth, some corraloids	partial moss covering	4	32.1	73
28	Cylindrical, with a bulbous tip	5	~15	25	12	<2°	S-SE	reminiscent of sand-paper	algal coating	n/a	31.3	75
9	2 fused stal., hole between, arched	5	4.3	180	75	25°	N-NE	entirely moss covered	moss, large plant, insects	41	32	73
8	Massive, bumpy, thin 30cm-long tip	5	4.1	180	150	<5°	N-NE	extremely bumpy, rough	moss, small plant, insects	54	32	73
29	Highly irregular, prong-like, 3 tips	7	~10	30	25	variable<30°	S-SW	smooth	moss, algae	n/a	30.3	80
7	Irregular, stubby	7	2.3	17	20	15°	S-SE	shaded smooth, lit part rough	moss, lichen, insects	2	32	73
6	Irregular, elliptical in cross-section, 2 tips	8	2	90	84	variable5-10°	S	smooth, some coralloids	moss, lichen, mud wasp	7	32.1	73
22	Irregular, attached to wall, projects out	8	5	60	60	variable <60°	S-SW	botryoidal, few coralloids	2 large plnts. moss, insects	24	30.2	79
26	Irregular, deflected stalactite	10	~12	20	30	<10°	S-SW	earthy, crusty	algal coating	n/a	31.5	75
27	Irregular, somewhat flattened	12	~15	15	14	<5°	S-SW	wet, pasty	thick, pasty algal coating	n/a	30.9	79
21	Changing deflection, defl. stalagm. below	12	2.1	150	80	variable<30°	S-SW	bumpy, earthy	luxuriant moss, insects	144	30	80
23	Irregular, attached to wall, soda straw	*17*	1.1	60	40	follows wall, soda straw <2°		small coralloids	algal coating at the tip	39	30	81
10	Regular, conical	*17*	1.7	35	12	vertical		reminiscent of sand-paper	none	<1	27.5	95
11	Irregular, flattened, partly curtain	*18*	2.4	60	60	variable <10°	S-SW	bumpy, crusty	algal coating, white fungus	6	31.5	77
12	Irregular, step-like, 3 soda straws	*21*	2	40	55	variable <35°	SW	smooth, earthy	light algal coating	65	31.4	78
5	Conical, slightly-arched	*22*	0.25	30	15	<5°	E-SE	wet, pasty organic coating	thick moss, black fungus	30	29.2	83
13	Irregular, step-like, bulbous	*23*	1	50	50	variable <35°	SW	smooth, flaky	algae (light), mud wasp	13	31.2	79
14	Several stalactites joined laterally	*27*	0.5	45	45	<2°	SW	rough, sharp coralloids	none	2	30.5	81
15	Cylindrical, abruptly narrow tip	*31*	1.5	27	14	<3°	SW	crumbly, some coralloids	algal coating at the tip	2	28.9	88
16	Conical, lowermost part of a pendant	**32**	0.7	60	40	vertical		rough, many coralloids	light greenish hue	14	29.2	86
17	Largely regular with a bulbous base	**30**	2.2	33	36	vertical		rough, few small coralloids	none	<1	27.6	91
18	Regular, elliptical in cross-section	**35**	2.1	35	21	vertical		smooth	none	<1	27.7	96
19	Almost perfectly conical	**36**	2	70	19	vertical		rough, lots of coralloids	none	17	28.6	96
20	Bulbous base with a thin stalactite	**41**	0.9	40	30	vertical		very rough to smooth	none	2	27.5	97
24	Conical, tip broken, new soda straw	**>45**	0.9	30	10	vertical		smooth	none (bats roost near)	47	27.9	94
25	Cylindrical, with 5 soda straws	**>45**	1.8	16	20	vertical		rough, lots of coralloids	none (bats roost near)	2	27	98

Note: Samples are arranged in the order of increasing distance from the dripline toward to the cave's rear. Numbers in the first column (#) are sample ID numbers, corresponding to locations indicated deposits in the outer entrance, inner entrance to innermost twilight zone area, and cave beyond the twilight zone). [b]H= height above ground. [c]L= maximum length. [d]C= maximum circumference. [e]Defle nally selected, but many dried out due to virtually no rainfall following 03/20 rain event. Drip rate was not measured for the five stalactites located in very high ceilings. [g]Rock type qualification is highl ed tufa and laminated tufa deposits respectively) and more solid deposits speleothems (abbreviated as Sm and S for microcrystalline speleothems and "normal" macrocrystalline speleothems respectively - aragonite with lesser calcite, A=C - aragonite and calcite in roughly equal proportions, C>A - calcite with lesser aragonite, C - mostly calcite. [i]Mud wasps (Hymenoptera: Sphecidae) often plaster thei

Microclimatic data			Rock desc.	
	4/9/04 at 12:00 noon			
air flow (m/s)	PAR (mmol/m²/s)	LI (lx)	phys. type[g]	XRD min.[h]
0.4	167	1378	Te	A=C
0.2	173	54	Tl	A>C
0.4	22	926	Tl	A>C
0.4	144	1055	Tl	A<C
0.2	148	1055	Te	A<C
0.2	38	861	Te	A=C
0.4	88	603	Te	C>A
0.4	93	603	Tl	A>C
0.2	17	807	Tl	C>A
0	69	527	Te	C>A
0	59	527	Te	A>C
0	31	1378	Te	C>A
0.2	11	646	Tl	A=C
0	16	667	Te	C
0	15	850	Te	A=C
0	1	78	Tl	C>A
0	0	0	S	A>C
0	8	205	Tl	A=C
0	4	97	Tl	A>C
0	3	43	Sm	C>A
0	2	11	S	A=C
0	1	5.4	Sm	A>C
0	0	2.2	S	A=C
0	0	1.1	S	A
0	0	0	S	A>C
0	0	0	Tl	A>C
0	0	0	S	A>C
0	0	0	S	A
0	0	0	S	A>C
0	0	0	S	A=C

l on Figure 2. [a]D= distance from the dripline (normal font, italic font, and bold font respectively indicate ection direction is italicized if prominently away from the light. [f]All stalactites were dripping when origi- y subjective. We chose to call friable microcrystalline deposits tufa (abbreviated as Te and Tl for encrust- y). [h]Mineralogy as determined by XRD analyses. Abbreviations are as follows: A - mostly aragonite, A>C r mud-cell nests to stalactites.

cliff causes minor spatial discrepancies in light levels in the cave's outer entrance zone (Fig. 4, see transect), and also accounts for somewhat patchy distribution of vegetation in the area (Fig. 4, inset). At the cave's inner entrance, enough light penetrates to allow human eyes to see quite well, but the availability of wavelengths suitable for photosynthesis is attenuated to less than 2% of open sky levels. This roughly coincides with the extinction of autotrophic biofilms that coat the rock surfaces in the cave's outer entrance and progressively diminish inward. Photosynthetically active radiation extinguishes some meters sooner than all visible wavelengths. Nonetheless, we have seen that the measurements of irradiance by normal light meters well approximate PAR levels (Fig. 4, see transect).

Airflow in the cave was evaluated because it is known to have an effect on stalactite morphology (Hill & Forti 1997). In cave entrances, in particular, where the growth axis of stalactites is commonly not vertical, air currents are sometimes suggested as one reason for deflection (e.g., Sevenair 1985). At our study site, however, no airflow into and out of the cave was registered. Minor air movement was occasionally detected in the outer entrance area, but its direction was usually along the outside cliff face (Fig. 4).

PROPERTIES OF STALACTITES

All specimens considered in this study are stalactitic in appearance and can clearly be referred to as stalactites. Nevertheless, they form a highly disparate set (Table 1), exhibiting divergent morphologies and a considerable number of distinct fabrics. They range from the highly irregular and crumbly stalactitic features in the most exposed locations to ordinary-looking speleothems found deeper inside the cave (see Table 1: Physical description). The greatest contrast exists between deposits in the outermost and innermost parts of the cave (see Table 1: Position), whose rock types correspond to calcareous tufa and normal speleothem travertines, respectively. The studied deposits are described here, in the "order of appearance" when entering the cave, in terms of external macromorphology, surface textures, internal macromorphology, and fabrics.

EXTERNAL MACROMORPHOLOGY

In Krabi area and similarly humid tropical karsts elsewhere, "stalactites" can grow outside of caves, and are prolific on limestone towers and cliffs. Despite their convincingly stalactitic appearance, however, these deposits are distinct from and are not to be considered true speleothems. They form in essentially epigean settings (Taboroši *et al*. 2004a), including transitional environments (e.g., shelter caves, cave entrances) and are ubiquitous in the humid tropics (Lehmann 1954, Wilford & Wall 1964, Longman & Brownlee 1980, Crowther 1982, Taboroši 2002). In Pop Kan Mai Cave they dominate the outermost parts, and range in size from a centimeter to meter scale (see Table 1: Size; but comparable deposits reaching tens of meters occur elsewhere in the Krabi area, most notably Rai Lay peninsula cliffs). The overall mor-

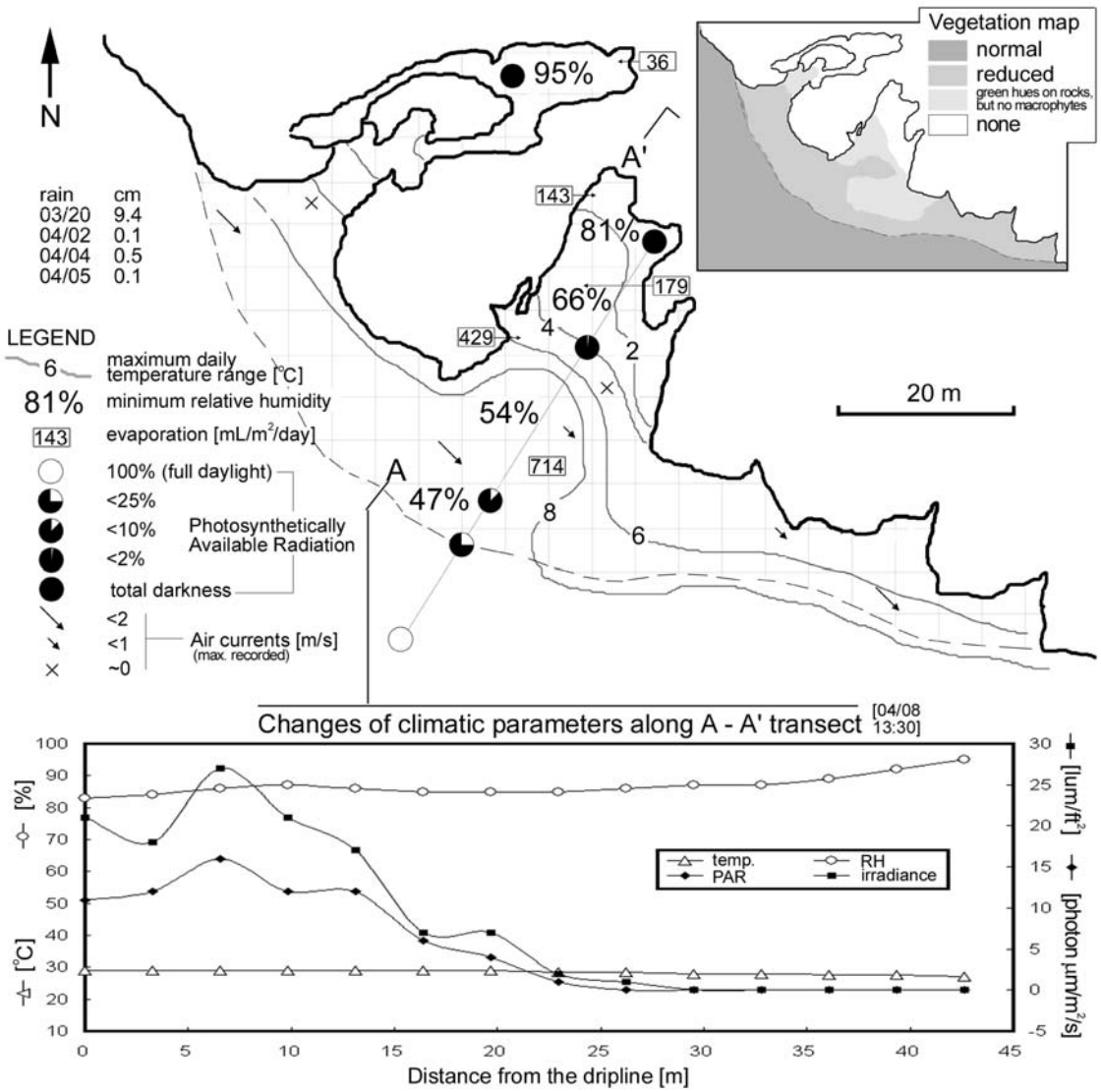

Figure 4. Microclimate map of Pop Kan Mai Cave, depicting approximate daily temperature ranges, minimum relative humidities, evaporation rates, PAR light levels, and predominant air currents. Inset map illustrates vegetation distribution, and the graph shows changes of climatic parameters along a transect from the entrance to cave interior.

phologic aspect of these "stalactites" is erratic, and shapes ranging from slightly asymmetrical (Fig. 5A) to highly irregular, such as bulbous, pendant-like, club-like, flattened, slanting, step-like, branching, and variously contorted forms are the norm. They can also be quite thin and elongated (Fig. 5B), but soda straws do not form. Growth is naturally guided by gravity, but is not entirely controlled by it, and deflections of growth axes are common (Fig. 5C). Tilting is often, but not necessarily, in the direction of light, and can be so pronounced as to approach horizontal growth in some locations. While most of the non-vertical growth is surely due to biologic processes, it cannot always be attributed simply to the preferential calcite deposition on light-facing sides by photosynthetic microorganisms, as generally suggested (e.g., Bull & Laverty 1982). Photo-orientation is, indeed, a common trait of epigean and cave entrance stalactitic deposits, and many of our samples clearly face the direction of sunlight. However, deflections are certainly caused by more complex imbalances in microbial biofilm dynamics, as suggested by the presence of deposits exhibiting inconsistent curvatures (Fig. 5C), specimens leaning away from the light, and adjacent stalactites slanting in conflicting directions (see Table 1: Deflection).

Further inward, in much of the twilight zone, stalactites are less lopsided than those in the more exposed areas. Many of them mimic the recognizable cylindrical and conical shapes of normal stalactites, but retain some irregularities. Generalizations are difficult due to the great variety of forms, but common shapes include somewhat globular, bent, and stunted (Fig. 5D) features, deflected deposits ranging from conspicuously step-like (Fig. 5E) to slightly bowed (Fig. 5F), and ordinary-looking stalactite bases with bulbous or disproportionably thin and elongate tips (Fig. 5G). When deflections are present, orientation towards the daylight source, as opposed to any direction, appears to be the rule and is most likely elicited by the dramatically reduced availability of PAR light. Another feature that contrasts these stalactites with their counterparts forming in more exposed parts of the cave is that they frequently have slight, often multiple, soda straws attached (often deep green or black due to microbial colonization).

Table 2. Descriptive statistics for the microclimate of Pop Kan Mai Cave. Note that maximum humidity levels experienced at the dripline (and probably outside the cave as well) are comparable to those deep inside the cave. This is certainly one of the factors allowing stalactite growth in epigean settings in the tropics. Also note that data logger 2 exhibits a greater temperature range and maximum value than logger 1, even though it was placed more inward from the dripline. This is probably due to uneven shading by the canopy.

Cave area	Outermost dripline	Outer entrance	Twilight zone front	Twilight zone rear	Cave interior
Data logger ID	1	2	3	4	5
Temperature (°C)					
Mean	27.3	27.3	26.7	25.9	25.1
Minimum	23.6	23.2	25.2	25.2	24.8
Maximum	31.1	31.5	28.3	26.7	25.2
Range	7.5	8.3	3.1	1.6	0.4
Standard deviation	1.8	1.9	0.6	0.3	0.1
Variance	3.1	3.6	0.4	0.1	0.0
Coeff. of variance	6.4	6.9	2.3	1.2	0.5
Relative humidity (%)					
Mean	83	87	90	95	99
Minimum	47	54	66	81	95
Maximum	96	97	96	98	100
Range	49	43	29	18	5
Standard deviation	9	9	4	3	1
Variance	79	74	19	7	2
Coeff. of variance	11	10	5	3	1
Data logger ID	A	B	C	D	E
Light intensity (lx)					
Maximum	275.5	212.1	12.9	0.0	0.0

Proceeding deeper into the cave, in the inner parts of the twilight zone and beyond, the morphology of stalactites gradually becomes no different from typical speleothems known from elsewhere. Reaching about 1.5 meters in length, they exhibit the familiar conical shapes (Fig. 5H), well developed soda straws, and strictly vertical growth axes (Fig. 5I).

SURFACE TEXTURES

The outer surfaces of stalactitic deposits in areas exposed to daylight exhibit a unique "organic" feel and distinctive pale to deep dark green, brownish, gray, and black coloration (Fig. 5A). Specimens found in the most exposed portions of the cave (as well as those outside it) are covered by moist and velvety coatings of algae, lichens, and especially mosses (Fig. 5B; 5C; also see Table 1: Exterior surface). In some cases, these outside layers can be dry and exhibit desiccation cracks, wrinkles, and flaking. Such dehydrated stages are probably a part of the annual cycle. Also evident can be roots of higher plants, which grow nearby or emerge from the stalactites themselves (Fig. 5B).

Further into the twilight zone, the obvious growths of bryophytes and higher plants are replaced by epilithic microbial biofilms, resulting in wet and pasty or powdery or earthy coatings (Fig. 5D; 5E; 5F). These organic layers can vary significantly in composition, causing sundry coloration: white, gray, yellowish, light to dark green and brown, purplish, and black. The biofilms are particularly pronounced on the sides facing the light (Fig. 5E), and support prolific colonies of prokaryotes and microphytes. The portions of the stalactites facing the darkness of the cave generally lack such biologic consistency and their surfaces are flat and smooth, rough or botryoidal, or exhibit jagged coralloid textures.

In the innermost twilight zone and deeper into the cave, significant biofilms gradually diminish, receding to the most damp areas near the stalactites' growing tips (Fig. 5G) and eventually dying out. As abiotic surfaces take over, stalactites gradually gain the crystalline luster of typical speleothems. They are colored white, yellowish, light gray, or brown, and their most common textures are coralloid, slightly rough (Fig. 5H), and smooth surfaces (Fig. 5I).

INTERNAL MACROMORPHOLOGY

Internal structure of stalactitic deposits found around the dripline is in stark contrast with usual cave speleothems. They are generally lightweight, porous, and friable, and many are weak enough to be plucked by hand. When broken, they reveal vuggy interiors, white to gray or brown, and composed of mouldy or layered calcareous tufa. They often contain soil and plant material (Fig. 6A), and almost invariably lack sparry crystals. Some of the most typical structures result from bryophyte encrustation and are composed of extremely porous spongy frameworks which may entirely lack (Fig. 6B) or display only rudimentary layering (Fig. 6C). Also common are laminated tufa deposits, which may be combined with encrusted fabrics (Fig. 6D) or concentrically layered and homogeneous, but nonetheless highly porous (Fig. 6E). Finally, in some cases, the laminae are surprisingly fine and ordered and convincingly resemble normal speleothems, but the deposits crumble easily and are fragile and powdery, reminiscent more of chalk than travertine (Fig. 6F).

Inside much of the cave's twilight zone, stalactites are denser and less porous than their analogues from the more exposed locations, but are still generally flimsy and can contain prominent voids (Fig. 6G). Classification is difficult due to the great diversity of morphologies and fabrics exhibited by individual specimens, but mostly microcrystalline makeup, with fairly irregular layering and some coarsely crystalline calcite, is the norm recognizable in most hand samples (Fig. 6H). Essentially, these deposits are transitional forms between the extremely irregular epigean tufa stalactites and normal cave speleothems. Some specimens can be heterogeneous, exhibiting discrepancies between light-facing sides (more tufa-like) and darkness-facing portions (more speleothem-like). In general, the former are vuggy and less organized, whereas the latter are denser and evenly laminated.

Further into the cave, stalactites are progressively dominated by solid, regular, concentrically layered coarsely crystalline structures (Fig. 6I). At the rear parts of the twilight zone, the

familiar dense laminae and sparry crystals are the standard composition, although some micritic material remains locally enclosed. The latter gradually recedes in specimens beyond the twilight zone, as stalactites assume the macrocrystalline make-up and consistent structure of typical speleothems.

STALACTITE FABRICS

Petrology of the stalactites we investigated is extremely varied. Containing both calcite and aragonite, they exhibit a bewildering array of fabrics, which contrast considerably among, but also within, individual specimens. As a preliminary classification, they can be broadly grouped into predominantly microcrystalline and macrocrystalline fabrics, in the order of progression from the most exposed to best enclosed parts of the cave (Table 3).

In general, microcrystalline fabrics correspond to calcareous tufa (or rather, an unusual subaerial, stalactitic form of it) and many are comparable to those well known from aquatic, traditional tufa deposits. They characterize the relatively open and microclimatically variable parts of the cave, with encrusted macrophyte fabrics (Fig. 7A; 7B) dominating the most exposed areas, and encrusted microbial fabrics (Fig. 7C; 7D) and amorphous (Fig. 7D; 7E) and laminated microcrystalline fabrics (Fig. 7E; 7F) typifying the twilight zone. In the inner reaches of the twilight zone, the fabrics become progressively ordered, less porous, and gradually dominated by spar (Fig. 7G; 7H). Within the stable and humid conditions beyond the twilight zone, the fabrics come to reflect ordinary speleothems (Fig. 7I).

The end member found in the cave's outermost parts is encrusted fabrics almost entirely bioconstructed by calcite precipitation on plant structures. They develop by deposition of microcrystalline $CaCO_3$ on exposed plant surfaces, resulting in highly porous (exceeding 90% porosity) fragile structures. A representative example is extremely vuggy lace-like networks (Fig. 7A) that have evidently formed by encrustation of bryophytes, which colonize vadose water drip points and whose living shrubs continue to grow as older parts become incorporated into incipient stalactitic deposits. The characteristic morphologies display well-defined molds and remains of moss stems and protonema (which also occur within other fabrics; Fig. 7E - top right) and are quite comparable to biogenic fabrics observed in conventional tufa (e.g., Weijermars *et al.* 1986). Similarly irregular, porous and easily recognizable tufa fabrics (Fig. 7B) form when hanging plant roots influence and guide the deposition of calcite by providing support and nucleation sites (resulting in tufaceous equivalents of cave rootsicles; see Taboroši *et al*. 2004b).

Microbial structures can also become encrusted by calcite (Fig. 8A), resulting in yet another series of distinct fabrics. One of the most fascinating encrusted microbial morphologies develops by calcification of colonies of filamentous cyanobacteria (Fig. 7C), which grow on the surfaces of stalactites reached by sufficient light to enable photosynthesis. Calcite is precipitated on the surfaces of cyanobacterial filaments, creating hollow tubes surrounded by one to several layers of calcite. Groups of filaments may be oriented along consistent axes or be randomly tangled, and the pore space between them may be empty or infilled by secondary calcite. In addition to filamentous cyanobacteria, numerous other calcified and uncalcified microbes and microbial structures (Fig. 8B) are exceedingly common in the twilight zone.

Alongside encrusted morphologies, stalactitic deposits at the entrance and in the twilight zone comprise other microcrystalline fabrics, both amorphous and layered. Amorphous fabrics are characterized by microcrystalline groundmass (Fig. 7D; 7E), often with interspersed organic-rich material (Fig. 7D), microbial structures (Fig. 8C; 8D), detrital grains and interred invertebrate and plant fragments (Fig. 7E–top right). Pore spaces can be infilled partly or completely by secondary calcite and aragonite (Fig. 7E–bottom right). Layered fabrics are analogous to laminated tufas and appear as highly porous layers of optically unresolvable crystallites (Fig. 7F). In many specimens, the white or transparent microcrystalline laminae are intercalated with brown and opaque organic material (Fig. 7F; 7G). Equivalent structures recognized by Chafetz & Meredith (1983), Chafetz & Folk (1984) and Folk *et al*. (1985) in various travertine deposits are attributed to bacterial activity. The laminae are seldom regular as in normal stalactites, and are generally undulatory, convoluted, and even discontinuous. They can also include layers of microsparitic or sparry calcite flanked by microcrystalline laminae, producing polycyclic spar/micrite couplets (Fig. 7G). This arrangement, as well, has been previously reported from normal, aquatic tufas (e.g., Jannsen *et al*. 1999, Pavlovic *et al*. 2002).

As the distance from the entrance increases, biogenic and amorphous structures become rare, and most deposits are organized as concentrically layered microcrystalline aggregates (Fig. 8E). They are progressively less porous and more orderly, exhibiting greater proportions of macrocrystals while retaining some microcrystalline material (Fig. 7H; 8F; 8G). Beyond the twilight zone, most fabrics are composed of equant and columnar calcite and acicular aragonite, initially poorly arranged (Fig. 8H) but progressively better organized and densely layered. They come to contain no significant microcrystalline or organic material and reflect quintessential speleothems (Fig. 7I; 8I).

DISCUSSION

CAVE MICROCLIMATE

Climatic data from tropical caves are limited, as the majority of relevant research was carried out in temperate regions. In the most comprehensive bibliography of spelean microclimatology to date only a few references are related to tropical caves (see Wefer 1991 and references therein). The distinctiveness of tropical cave microclimates as opposed to those of temperate caves was examined by Gamble *et al*. (2000). By identifying a number of idiosyncrasies that may be unique to tropical caves, they showed that extant cave microclimate

models may not be applicable in the tropics. The microclimatic observations reported in this paper and data from previous work (Taboroši & Hirakawa 2003) generally conform to the conclusions of Gamble *et al*. (2000). Specifically, we have also found that external atmospheric variations project into a cave and diminish toward the rear, and that the deep cave microclimatic zone (Cropley 1965) can be missing due to small size of caves relative to their entrances. A significant difference, however, is that while Gamble *et al*. (2000) found warmer conditions in the back portions of caves, we recorded consistently cooler temperatures at the rear, both in Thailand, as well as in the Mariana Islands (Taboroši & Hirakawa 2003). While this may be a consequence of different monitoring periods and seasonal variations, it is more likely due to the differences in the caves' physical configuration, such as passage geometry and size and number of entrances, which are known to largely determine microclimate regimes of individual caves (de Freitas *et al*. 1982).

MICROCLIMATIC CONTROLS ON FORMATION OF STALACTITES

Since all the specimens we collected are from a single cave located in an isolated karst tower, we deem that all are fed by the same groundwater body overlying the cave and expect no major geochemical variations in their respective dripwaters. Although we did go into the field prepared to check dripwater *p*H and conductivity, the dry weather and slight drip-rates prevented us from taking meaningful measurements (as degassing and evaporation modified water chemistry during the days-long periods it took to acquire volumes sufficient for testing by hand-held meters). While documenting dripwater geochemistry remains an objective for future related research, we believe that the small size of the studied cave and its location in a discrete limestone tower imply that dripwater feeding all stalactites comes from a single perched and clearly delimited groundwater body, isolated from local input of any other vadose water. Therefore, we view the profound morphologic and petrologic differences among the studied specimens predominantly as the function of each stalactite's own microclimatic and ensuing biologic environment, determined by its specific position in the cave.

The general trend is that as diurnal variations are alleviated and humidity increased and stabilized, the deposits show progressively lower porosity and heterogeneity and greater crystal size and level of organization (Fig. 9). At the land surface, the effects of increased evaporation cause rapid precipitation of calcite from karst water, resulting in poorly arranged and randomly oriented microcrystalline aggregates. This is a well-known phenomenon influencing the fabric of calcareous tufa deposits worldwide (Ford 1989, Viles & Goudie 1990, Ford & Pedley 1992, 1996), but is generally not considered in the case of cave stalactites. Nonetheless, the irregular crumbly stalactites we observed in the most exposed parts of the cave are produced partly by this process, and essentially comprise a unique, subaerial category of tufa. In addition to increased evaporation, the precipitation of these deposits is affected by the pronounced diurnal, seasonal, and annual variations in temperature and humidity levels (as well as other indirectly-linked parameters such as changes in canopy abundance and shading effects). Due to these oscillations, calcite deposition is inconsistent and results in the observed heterogeneities in macromorphology and fabrics.

In better-enclosed settings, the relative humidity is increased and the variations in temperature and humidity are reduced, allowing the precipitation of progressively larger and more regular crystals and more consistent fabrics. This is manifested in stalactites that form in the cave's twilight zone and contain both microcrystalline and sparry calcite and aragonite. As the humidity levels increase and stabilize with distance inward from the cave entrance, the proportion of macrocrystalline to microcrystalline $CaCO_3$ is amplified and heterogeneities in the fabrics are reduced. Finally, as consistently high humidity levels are reached deeper inside the cave, the effects of evaporation are nearly eliminated, and the resultant deposits are composed of orderly coarsely crystalline fabrics precipitated by CO_2 degassing. Within such a microclimatically stable environment, variations in water availability and geochemistry are expected to overcome microclimatic (and biologic) factors as the primary controls of precipitated carbonate morphology.

BIOLOGIC CONTROLS ON FORMATION OF STALACTITES

Concomitantly with the physico-chemical precipitation, living organisms exert their influence on carbonate deposits. The mechanisms by which biota interact with sediments are numerous and still insufficiently known, but it is now generally accepted that most carbonate precipitates are shaped by biologic activity in addition to the inorganic processes, and many are almost entirely biogenic (Viles 1988). Since the presence of living organisms on any given substrate is controlled by environmental conditions, the gradients in temperature, humidity, and illumination in spelean settings translate directly into gradients in abundance, diversity, and species composition of local biota. Numerous studies have demonstrated that biologic diversity declines as a response to reduced light levels in caves (Piearce 1975, Cubbon 1976, Pentecost & Zhaohui 2001), which entails a decrease in biologic involvement in carbonate precipitation. Consequently, many epigean carbonates are often biogenic (Viles 1988) whereas most cave carbonates are considered abiotic (Thraikill 1976). This relationship is clearly visible in the cave we studied, where the patterns of microclimatic change from the entrance to interior are closely reflected by biology.

In the outermost, best-illuminated part of the cave, many stalactitic deposits are colonized by bryophytes and higher plants, and are consequently dominated by encrusted macrophyte structures. This encrustation process, driven by the photosynthesis-respiration cycles of the substrate plants (Pentecost 1996), is a well-known phenomenon in cascade and other classic tufas (e.g., Pavlovic *et al*. 2002), but is rarely documented in connection with stalactites. Only a few moss-encrusted

Table 3. Stalactite fabrics broadly grouped in the order of progression from the cave's most exposed to best enclosed parts. (See Fig. 9 for a schematic diagram.)

Stalactite Fabrics	Type	Position	Climate	Illumination
Microcrystalline fabrics		entrance	variable	normal
a) Encrusted macrophytes	tufa			
b) Encrusted microorganisms		cave		reduced
c) Amorphous microcrystalline		twilight	buffered	
d) Laminated microcrystalline	transitional	zone		
Macrocrystalline fabrics				minimal
a) Poorly organized, some microcrystalline	(travertine)			
b) Classic carbonate speleothem microfabrics	speleothems	interior	stable	none

"speleothems" have been described before (e.g., Lichon 1992, Zhaohui & Pentecost 1999), but their occurrence in the tropics is much wider than the occasional reports seem to suggest.

As light is reduced further into the cave, macrophytes disappear but photosynthetic microbes continue to thrive in complex epilithic biofilms. This is macroscopically apparent from the greenish hues on cave walls and especially on stalactites (which, being endpoints of vadose flow paths, are wet and preferentially colonized by organisms) and is also evident in stalactite fabrics, which commonly contain calcified filaments and microorganisms. In some cases, microbial colonies, notably obligatory calcifying cyanobacteria, are sole builders of some stalactites, as they provide the frameworks subsequently strengthened by secondary calcite precipitation in pore spaces (Taboroši & Hirakawa 2004). Unlike passive calcification by macrophytes, which is generated by photosynthetic modification of the medium and leads to spontaneous precipitation (e.g., Weijermars *et al*. 1986), microbial calcification is thought to be a more active process, or rather, a suite of processes (e.g., Pedley 1994). Cyanobacteria, for example, are thought capable of initiating and controlling the precipitation (Pentecost & Riding 1986, Merz 1992, Schneider & Le Campion Alsumard 1999), and so are other microbes (e.g., Chafetz & Folk 1984).

Specialized autotrophic microorganisms are capable of photosynthesis even at extremely low light levels (Cox & Marchant 1977) and persist deep into the twilight zone. Nevertheless, overall photosynthesis is dramatically reduced with distance from the entrance, which leads to a loss of biodiversity and complexity of epilithic biofilms and their relative participation in the formation of secondary carbonate deposits. This is apparent from the fabrics of stalactites in the twilight zone: they retain some evidence of calcified microbes and biologically precipitated material, but steadily transition to more abiotic microcrystalline and macrocrystalline deposits. Although certain chemotrophic and heterotrophic microorganisms can impact the formation of speleothems deep within the spelean realm (Northup et al. 2000, Jones 2001), most carbonate precipitates in the complete darkness of caves are considered "absolutely inorganic" (Forti 2001) and we have seen no evidence of microbes in stalactites beyond the twilight zone.

The fact that living organisms can directly control the fabrics of stalactites we studied should not lead to underestimating the importance of the microclimate. In fact, the succession in biologic involvement in precipitation is a reflection of the microclimatic gradient (Fig. 9), with which it is intricately linked. Microclimatic variations, and especially different illumination levels, define the ability of specific microorganisms to colonize a particular substrate, and thus determine the nature of epilithic biofilm that develops on a given surface (Taboroši & Hirakawa 2004). This, in turn, impacts carbonate precipitation and influences the incipient deposits. In effect, the mor-

Figure 5 (next page). Stalactitic deposits *in situ*, including those in the outer entrance (A-D), twilight zone (E-G), and innermost twilight zone and beyond (H-I). Sample ID numbers of illustrated specimens are indicated in brackets. A) A slightly arched stalactite growing just a few meters from the dripline. Its monotonous gray color is due to a pervasive powdery biofilm [9]. B) Stalactites adjacent to the previous specimen. Note the irregularities such as non-vertical growth, inconsistent width, and an elongate tip. Stalactite in the foreground is dark due to a thorough moss cover. Note the large plant rooted in the stalactite itself [8]. C) A stalactite that starts as a drapery and grows on a cliff wall, in a very open location. Note its bent shape due to a changing growth direction, and a luxuriant moss cover (dark) on its light facing side [21]. D) A stunted stalactitic deposit, covered by thick, but largely dry and flaking, organic coating [6]. E) A stalactite inside the cave's twilight zone. Its step-like growth faces the entrance [12]. F) Twilight zone stalactites, with hooked shapes and covered by copious gooey organic material [5]. G) A cylindrical stalactite with a disproportionately narrow tip. Only the moist tip is colonized by a lush microbial biofilm (dark-colored and in stark contrast with the rest of the deposit) [15]. A rough-surfaced stalactite in the innermost reaches of the twilight zone [16]. I) Archetypal stalactites and soda-straws in the rear of the cave [17].

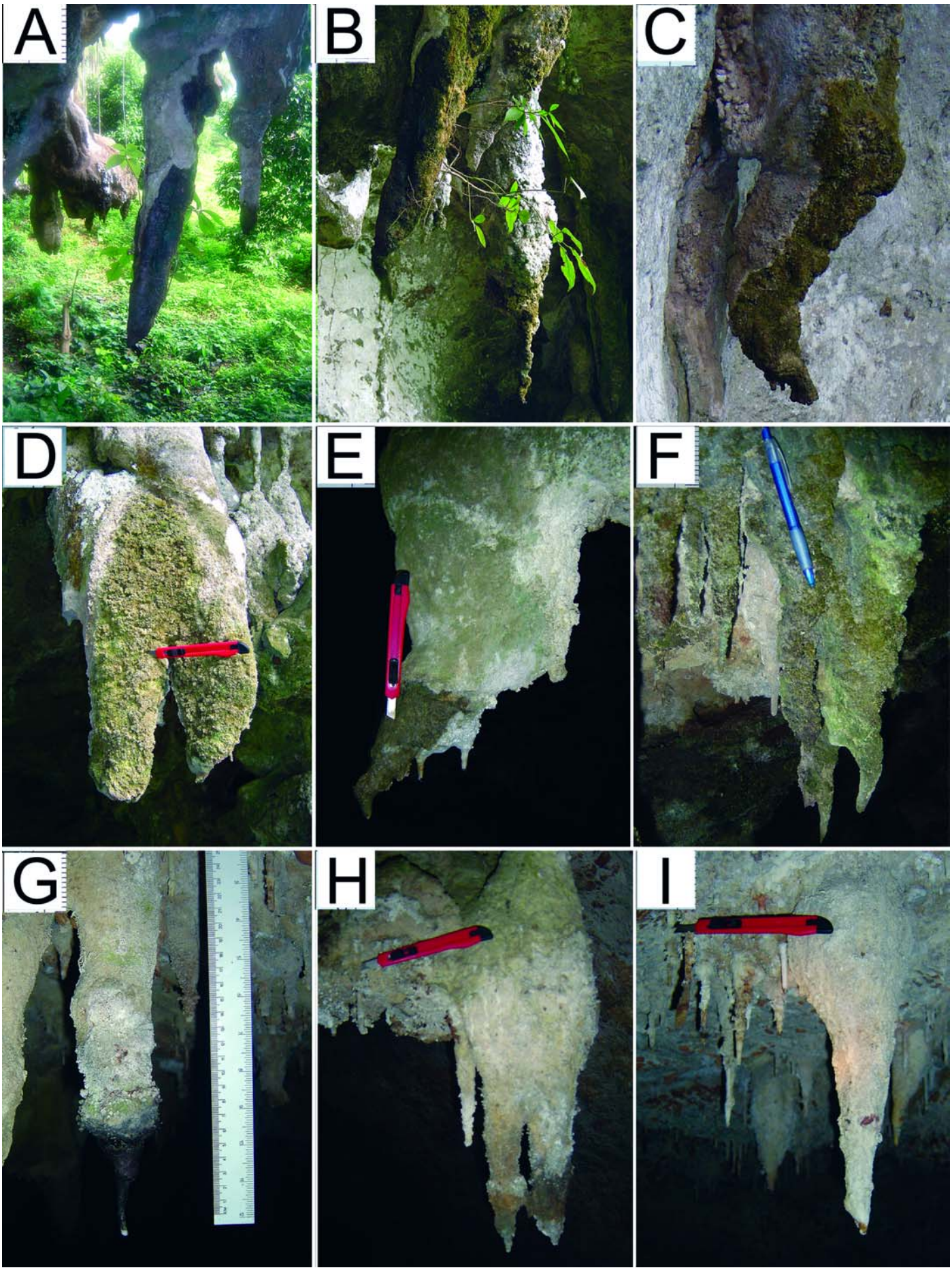
A
B
C
D
E
F
G
H
I

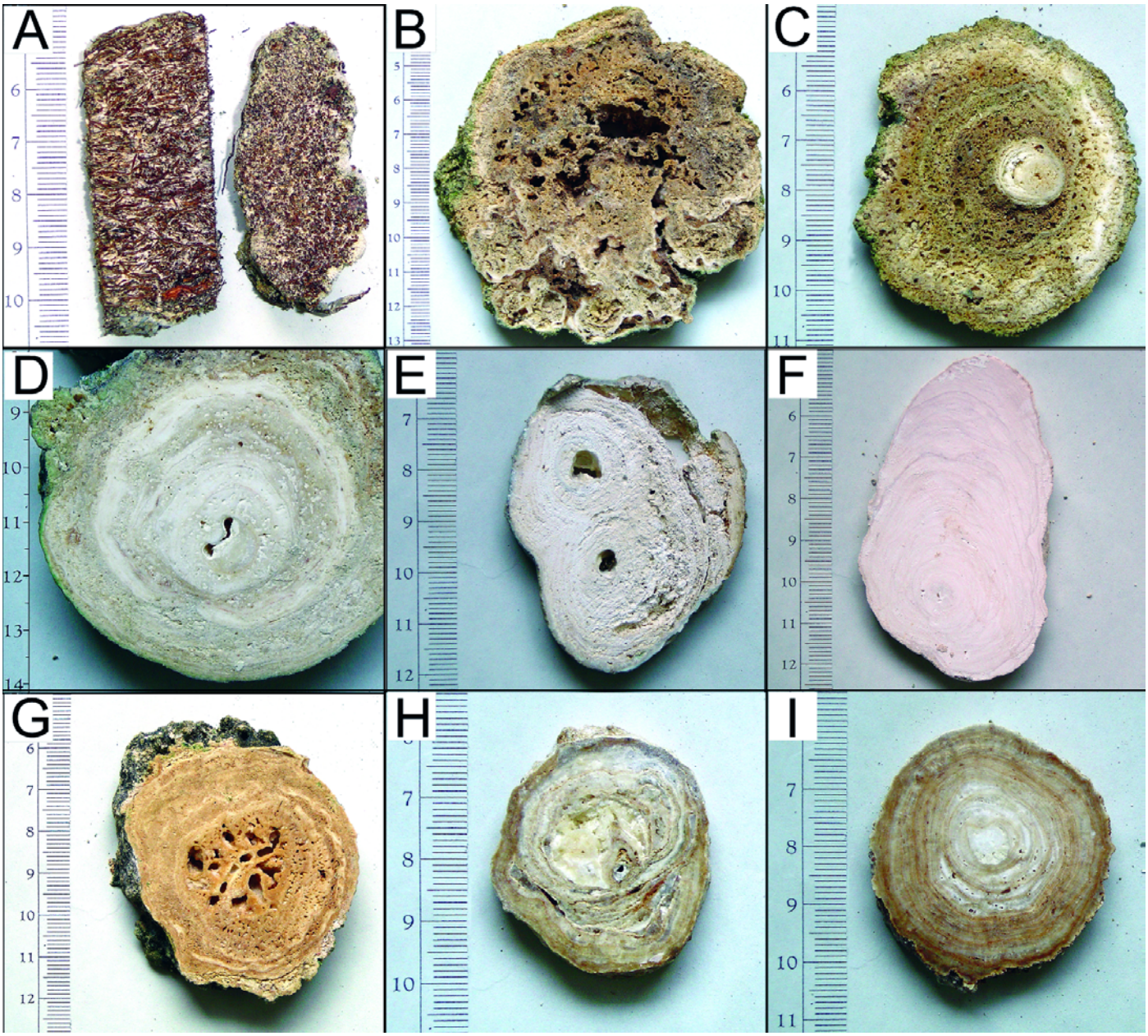

Figure 6. A series of cross-sections of stalactites approximating a transect from the entrance to the interior of the cave, consisting of encrusted (A-D) and layered microcrystalline (D-F) fabrics, transitional specimens (F-H) and a normal speleothem (I). Scales in centimeters. Sample ID numbers of illustrated specimens are indicated in brackets. A) An extremely fragile fragment formed by encrustation of hanging plant roots [9]. B) A highly porous, spongy stalactite formed by bryophyte encrustation [21]. C) A visibly layered bryophyte-encrusted feature, formed by moss colonization of an incipient microcrystalline stalactite (deposit core) [28]. D) A laminated tufa stalactite with outermost parts composed of encrusted material [8]. E) A regularly layered and homogeneous, but nonetheless highly porous, tufa stalactite exhibiting no macrophyte encrustation [4]. F) An extremely finely laminated, chalk-like microcrystalline stalactite resembling a normal speleothem but displaying no spar whatsoever [18]. G) A hard, concentrically layered microcrystalline deposit, exhibiting convoluted laminae and macroporosity [14]. H) A stalactite composed of microcrystalline material and spar crystals, arranged in somewhat irregular laminae [24]. I) A hard, dense macrocrystalline stalactite composed of regular, finely layered concentric laminae [19].

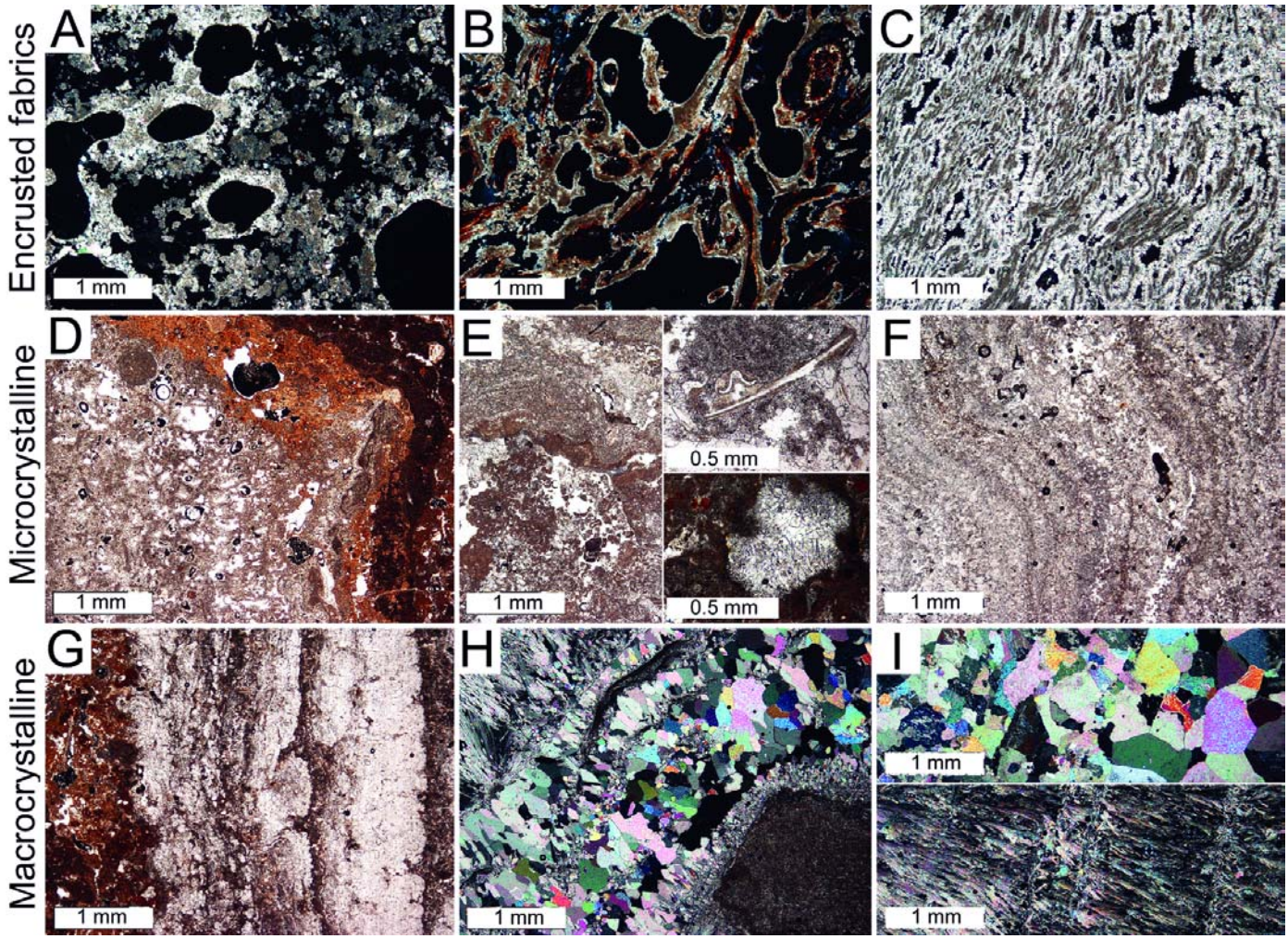

Figure 7. Thin-section micrographs of fabrics characterizing the range of stalactites from cave entrance to interior, including encrusted (A-C), amorphous (D-E) and laminated (F-G) microcrystalline, and partially (H-I) and completely (J) macrocrystalline fabrics. Note that all micrographs (except the two insets) were taken at the same magnification. Sample ID numbers of illustrated specimens are indicated in brackets. A) An extremely porous deposit formed by bryophyte encrustation [21]. B) An analogous feature formed by encrustation of hanging plant roots [9]. C) A fabric comprised of calcified cyanobacterial filaments [27]. D) A microcrystalline deposit comprised of calcified microbes (light material), amorphous organic-rich mass (dark), and numerous detrital grains [26]. E) Amorphous microcrystalline groundmass (left half) [22], moulds of moss stems and protonema (top right) [8], and pore spaces partially filled by secondary calcite and aragonite (bottom right) [28]. F) A porous, laminated deposit composed of microcrystalline material and some detrital grains (black) [11]. G) A laminated deposit composed of intercalated laminae of microcrystalline and organic-rich material (dark layers) and larger crystals (light layers) [10]. H) A complex deposit typical of the twilight zone, where microcrystalline material (lower right) is in close association with macrocrystalline calcite (middle) and aragonite (top left) [15]. I) Typical speleothem fabrics composed of homogeneous, well-organized equant calcite (top) [25] and acicular crystals of aragonite (bottom) [20].

phology and petrology of stalactites are a function of environmental factors by two parallel pathways: microclimatic variations directly influence carbonate precipitation; and also determine the composition and dynamics of biologic communities, which then influence carbonate precipitation in their own right.

DIAGENETIC CHANGES AND IMPLICATIONS TO PALEOENVIRONMENTAL INTERPRETATIONS

We have demonstrated that morphologic properties of stalactites are partly determined by the microclimate in which they are deposited, and that specific fabrics can be correlated to different temperature, humidity, and illumination regimes. This can be a useful tool in the interpretation of former environments and microclimates. For example, an excellent paper

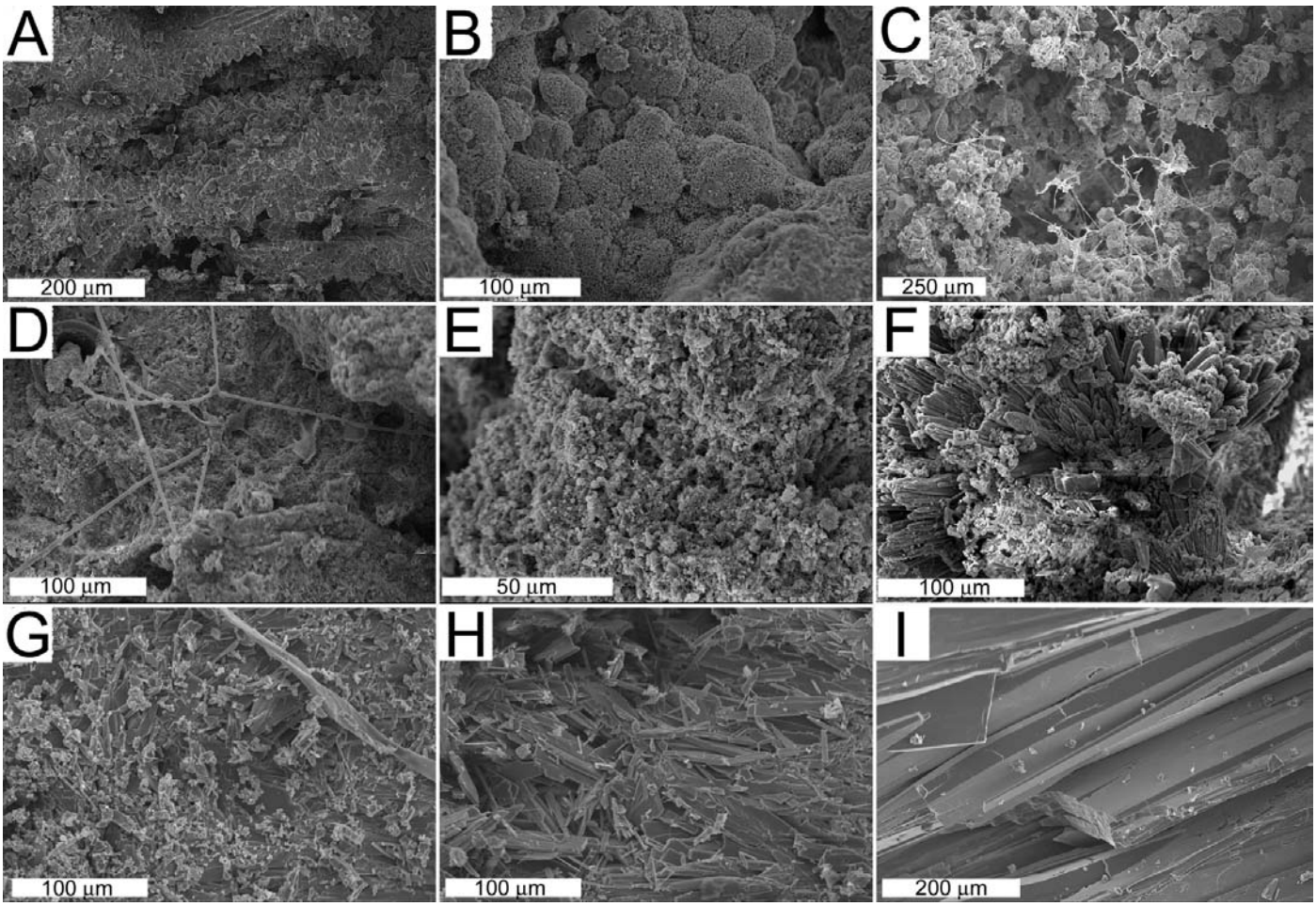

Figure 8. SEM micrographs of stalactites from cave entrance to interior. Sample ID numbers of illustrated specimens are indicated in brackets. A) Rod-like structures formed by encrustation of microbial filaments [4]. B) Shrub-like structures thought to be produced by microbial calcification [1]. C) Highly porous matrix of crystallites entangled in filamentous organic structures [30]. D) Microcrystalline substrate with copious microorganisms [9]. E) Microcrystalline aggregate lacking apparent microbial structures [22]. F) Small columnar crystals of calcite combined with much microcrystalline material [11]. G) Poorly organized macrocrystals interspersed with some crystallites and an organic filament [15]. H) A homogeneous deposit consisting solely of poorly arranged calcite crystals [18]. I) Solid columnar calcite structure of a typical speleothem [25].

by Jones & Motyka (1987) describes stalactites from the Cayman Islands, unusual in the fact that they are composed of biogenic structures and microcrystalline calcite. The stalactites are inactive, broken deposits from "ancient, filled caves," now embedded in calcarenite. Given descriptions by Jones & Motyka (1987), we believe the stalactites in question correspond to intermediary fabrics between subaerial tufa and normal speleothems and would have formed in a microclimatically transitional environment, rather than a well enclosed cave. The location where they were found, therefore, probably corresponds to cave entrance facies.

In addition to helping identify former microclimatic and geomorphic settings, petrologic idiosyncrasies of stalactites can indicate microclimate changing events, for instance breaching and collapse of caves. Such events cause shifts in local microclimatic gradients and force the actively forming speleothems to equilibrate with the new conditions. We have seen deposits that had started as normal stalactites but later abruptly assumed deflected growth and continued forming as tufa (most likely as a result of cave breaching), and suppose that opposite sequences could also be produced (e.g., by blocking of entrances by collapse). Dating of the different fabrics could pinpoint the timing of such events.

However, there are some important considerations regarding the use of stalactites in paleoenvironmental interpretation. As emphasized at the beginning of this paper, petrologic properties of stalactites are affected by both microclimatic conditions and the properties of the water from which they are precipitated. As a result, it is not unlikely that different mechanisms can, under specific conditions, produce comparable

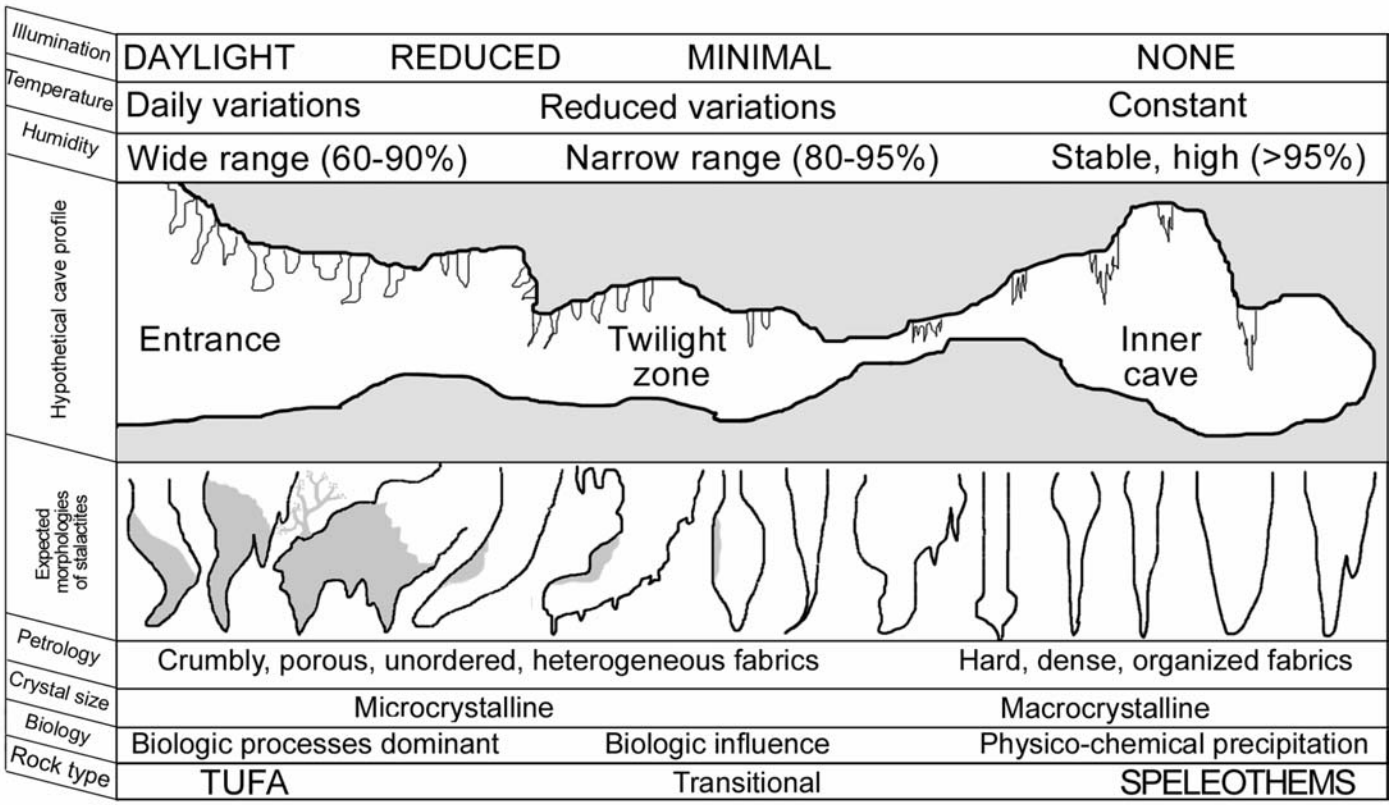

Figure 9. A schematic diagram of a hypothetical cave, showing expected microclimatic patterns and the likely characteristics of stalactites forming the range from irregular, microcrystalline tufa deposits at the cave entrance to normal speleothems at the back. The illustrations of expected stalactites illustrate diversity of morphologies, not progression. Predictable moss-covered surfaces are shown in dark gray. (Modified from Taboroši & Hirakawa 2003).

depositional fabrics. Microcrystalline stalactite fabrics are known to occur deep in some caves and even calcareous tufa—an intrinsically epigean deposit whose precipitation is controlled by environmental and biologic factors normally found at the land surface, can be, in rare instances, produced in spelean settings, from water under geochemical disequilibrium conditions (Frisia *et al*. 2000). Even more importantly, carbonate deposits can be profoundly altered by diagenesis, which sometimes obliterates original calcite fabrics. For instance, tufa is known to recrystallize into coarsely crystalline calcite, losing much of the biologic structure in the process (Love & Chafetz 1988, Pedley 1987). Conversely, tufa-like stalactites could conceivably form by decay and diagenesis of true cave speleothems, if the latter are exposed at the land surface conditions by cave collapse, as suggested by Bar-Matthews *et al*. (1991). Transformation of sparry calcite into micrite is known to occur (e.g., Jones & Pemberton 1987, Chafetz & Butler 1980, Chafetz *et al*. 1994), although there is no evidence that this is a wide-ranging process capable of transforming entire stalactites. Jones (1987), for example, observed spamicritization in just the top few microns from the rock surface in Oligocene-Miocene limestone in a humid tropical climate, while Hill and Forti (1997) mention chalkified layers up to 3 cm deep on the surfaces of old, inactive speleothems.

Therefore, reliable use of stalactite fabrics in paleoenvironmental interpretation requires an improved understanding of the extent to which diagenetic changes occur on stalactites, and ways to distinguish between diagenetically-altered fabrics and the primary depositional fabrics which they may mimic.

CONCLUSION

In their review of tufa and travertine deposits of the world, Ford & Pedley (1996) suggested that speleothems may be considered an "inorganic end-member of a continuum which, at the other extreme is represented by biomediated tufa." This continuum, however, has been largely theoretical, because typical tufas and speleothems develop in very different depositional environments that can hardly be spanned by actual intermediary forms. Because the overwhelming majority of tufa grows subaqueously in springs, rivers, lakes and swamps, whereas most speleothems form subaerially inside caves, the two are rarely exposed in the vicinity of each other and the continuum between them is based on an array of analogous fabrics, rather than any visible gradation of deposits in a given locale.

The most casual observations in tropical cave entrances reveal that stalactites are soft and fragile in the most exposed

locations, and more dense and solid in better-enclosed areas. A detailed look at a single cave in Krabi Province, Thailand, clearly demonstrated the full range of progressively denser and more organized deposits, from calcareous tufa stalactites at the dripline to classic speleothems deeper inside caves, and the veritable sequence of fabrics, from biogenic microcrystalline forms to densely layered travertines. While the most porous and friable "stalactites" at the land surface and in cave entrances exhibit much more in common with typical (aquatic) calcareous tufas than with speleothems, they are genetically clear analogues of spelean dripstone: just like their equivalents deeper inside caves, these stalactites are precipitated from epikarstic water dripping from bedrock ceilings. The underlying physical and chemical mechanisms involved in their precipitation are, thus, no different from normal cave stalactites, and it is the microclimate of their depositional setting and superimposed biologic processes that are responsible for the observed morphologic and petrologic idiosyncrasies.

ACKNOWLEDGEMENTS

We are grateful to Dr. John E. Mylroie (Mississippi State University), Dr. John W. Jenson (University of Guam), and Mr. Kevin Stafford (New Mexico Institute of Mining and Technology) whose collaboration over the years and numerous relevant discussions helped shape our ideas. We deeply appreciate the help of Mr. Mark Cartwright, Mr. Kevin Van Dusen, and Ms. Yukari Nakamura during fieldwork in Thailand and the kindness of the Thai family living in Chong Phli village, near the cave we studied. At Hokkaido University, we are thankful to Dr. Tomohisa Irino, Dr. Mitsuhiro Nakagawa, Dr. Hisatake Okada, Mr. Kesiuke Nagai, Ms. Akiko Matsumoto, and the faculty and students of the Geoecology Lab at the Graduate School of Earth and Environmental Science for their help and support. Finally, we are indebted to Dr. Bruce Railsback (University of Georgia) and Dr. Darlene Anthony (Purdue) whose reviews of the original manuscript helped improve this paper and gave us much encouragement.

REFERENCES

Atkinson, T.C. & Smith, D.I., 1976, The erosion of limestones, *in* Ford, T.D. & Cullingford, C.H.D., eds., The Science of Speleology: London, Academic Press, p. 157–177.

Bar-Matthews, M., Matthews, A. & Ayalon, A., 1991, Environmental controls of speleothem mineralogy in a karstic dolomitic terrain (Soreq Cave, Israel): J. Geol., v. 99, p. 189–207.

Borsato, A., Frisia, S., Jones, B. & Van Der Borg, K., 2000, Calcite moonmilk: crystal morphology and environment of formation in caves in the Italian Alps: Journal of Sedimentary Research, v. 70, p. 1171–1182.

Buecher, R.H., 1999, Microclimate study of Kartchner Caverns, Arizona: Journal of Cave and Karst Studies, v. 61, p. 108–120.

Bull, P. A. & Laverty, M., 1982, Observations on phytokarst: Zeitschrift für Geomorphologie, v. 26, p. 437–457.

Bögli, A., 1980, Karst hydrology and physical speleology: Berlin, Springer-Verlag, 284 p.

Chafetz, H. & Butler, J. C., 1980, Petrology of recent caliche pisolites, spherulites, and speleothem deposits from central Texas: Sedimentology, v. 27, p. 492–518.

Chafetz, H.S. & Folk, R.L., 1984, Travertines: Depositional morphology and the bacterially controlled constituents: Journal of Sedimentary Petrology, v. 54, p. 289–316.

Chafetz, H.S. & Meredith, J.S., 1983, Recent travertine pisoliths (pisoids) from southeastern Idaho, USA, *in* Peryt, T.M., ed., Coated grains: Berlin, Springer-Verlag, p. 450–455.

Chafetz, H.S., Rush, P.F. & Utech, N.M., 1991, Microenvironmental controls on mineralogy and habit of CaCO3 precipitates: an example from an active travertine system: Sedimentology, v. 38, p. 107–126.

Chafetz, H., Srdov, D. & Horvatinnic, N., 1994, Early diagenesis of Plitvice Lakes waterfall and barrier travertine deposits: Geographie Physique et Quaternaire, v. 48, p. 245–255.

Cox, G. & Marchant, H., 1977, Photosynthesis in the deep twilight zone: micro-organisms with extreme structural adaptations to low light, *in* Ford, T. D., ed., Proceedings of the 7th International Speleological Congress: Sheffield, British Cave Research Association, p. 131–133.

Cropley, J.B., 1965, The influences of surface conditions on temperatures in large cave systems: Nat. Speleol. Soc. Bull., v. 27, p. 1–10.

Crowther, J., 1982, Ecological observations in a tropical karst terrain, West Malaysia. J. Biogeog., v. 9, p. 65–78.

Cubbon, B.D., 1976, Cave flora, *in* Ford, D. T., & Cullingford, C. H. D., (eds.), The science of speleology: London, Academic Press, p. 423–452.

Dasher, G.R., 1994, On Station: A Complete Handbook for Surveying and Mapping Caves: Huntsville, Alabama, National Speleological Society, 242 p.

Dreybrodt, W., 1988, Processes in Karst Systems: Physics, Chemistry, and Geology: Berlin, Springer-Verlag, 288 p.

Dunkley, J.R., 1994, Thailand Caves Catalogue: Sydney, Australia, Speleological Research Council, Australian Speleological Federation, 44 p.

Dunkley, J.R., 1995, The Caves of Thailand: Sydney, Australia, Speleological Research Council, Australian Speleological Federation, 124 p.

Emeis, K.C., Richnow, H.H. & Kempe, S., 1987, Travertine formation in Plitvice National Park, Yugoslavia: chemical versus biological control: Sedimentology, v. 34, p. 595–609.

Folk, R.L., Chafetz, H.S. & Tiezzi, P.A., 1985, Bizarre forms of depositional and diagenetic calcite in hot-spring travertines, central Italy, *in* Schneidermann, N. & Harris, P.M., eds., Carbonate cements (Special Publication 36): Society of Economic Paleontologists and Mineralogists, p. 349–369.

Ford, D.C. & Ewers, R.O., 1978, The development of limestone cave systems in the dimensions of length and depth: Can. J. Earth Sci., v. 15, p. 1783–1798.

Ford, T.D., 1989, Tufa - the whole dam story: Cave Science, v. 16, p. 39-50.

Ford, T.D. & Pedley, H.M., 1992, Tufa deposits of the world: J. Speleol. Soc. Japan, v. 17, p. 46–63.

Ford, T.D. & Pedley, H.M., 1996, A review of tufa and travertine deposits of the world: Earth-Science Reviews, v. 41, p. 117–175.

Forti, P., 2001, Biogenic speleothems: an overview: International Journal of Speleology, v. 30A(1), p. 39–56.

de Freitas, C.R., Littlejohn, R.N., Clarkson, T.S. & Kristament, I.S., 1982, Cave climate: assessment of airflow and ventilation: J. Climatol., v. 2, p. 383–397.

Frisia, S., Borsato, A., Fairchild, I.J. & McDermott, F., 2000, Calcite fabrics, growth mechanisms, and environments of formation in speleothems from the Italian Alps and southwestern Ireland: Journal of Sedimentary Research, v. 70, p. 1183–1196.

Frisia, S., Borsato, A., Fairchild, I.J., McDermott, F. & Selmo, E.M., 2002, Aragonite–calcite relationships in speleothems (Grotte de Clamous, France): Environment, fabrics, and carbonate geochemistry: Journal of Sedimentary Research, v. 72, p. 687–699.

Gamble, D.W., Dogwiler, J.T. & Mylroie, J.E., 2000, Field assessment of the microclimatology of tropical flank margin caves: Climate Research, v. 16, p. 37–50.

Gams, I., 1968, Über die factoren die Intensität der Sintersedimantation bestimmen, *in* Proc. 4th International Congress of Speleology, v. 3, p. 107-15.

Given, R.K. & Wilkinson, B.H., 1985, Kinetic control of morphology, composition, and mineralogy of abiotic sedimentary carbonates: Journal of Sedimentary Petrology, v. 55, p. 109–119.

Gonzales, L.A., Carpenter, C.J. & Lohmann, K.C., 1992, Inorganic calcite morphology: roles of fluid chemistry and fluid flow: Journal of Sedimentary Petrology, v. 62, p. 382–399.

Harmon, R.S., Atkinson, T.C. & Atkinson, J.L., 1983, The mineralogy of Castleguard Cave, Columbia Icefields, Alberta, Canada: Arctic and Alpine Research, v. 15, p. 503–506.

Harper, S. B., 1999, Morphology of tower karst in Krabi, southern Thailand: Geological Society of America Abstracts with Programs, v. 31, p. A-52.

Hill, C. A. & Forti, P., 1997, Cave Minerals of the World: Huntsville, Alabama, National Speleological Society, 380 p.

Jannsen, A., Swennen, R., Podoor, N. & Keppens, E., 1999, Biological and diagenetic influence in Recent and fossil tufa deposits from Belgium: Sedimentary Geology, v. 126, p. 75–95.

Jennings, J. N., 1985, Karst geomorphology: Oxford, Basil Blackwell, 293 p.

Jones, B., 1987, The alteration of sparry calcite crystals in a vadose setting, Grand Cayman Island: Canadian Journal of Earth Science: v. 24, p. 2292–2304.

Jones, B., 2001, Microbial Activity in Caves: A Geological Perspective: Geomicrobiology Journal, v. 18, p. 345–357.

Jones, B. & Motyka, A., 1987, Biogenic structures and micrite in stalactites from Grand Cayman Island, British West Indies: Canadian Journal of Earth Sciences, v. 24, p. 1402–1411.

Jones, B. & Pemberton, S. G., 1987, The role of fungi in the diagenetic alteration of spar calcite: Canadian Journal of Earth Science: v. 24, p. 903–914.

Lehmann, H., 1954, Der tropische Kegelkarst auf den Grossen Antillen: Erdkunde, v. 8, p. 130–139.

Lichon, M.J., 1992, The phototropic phytospeleothems of Moss Palace, Mole Creek, Tasmania: Helictite, v. 30, p. 8–10.

Longman, M. W. & Brownlee, D. N., 1980, Characteristics of karst topography, Palawan, Philippines: Zeitschrift für Geomorphologie, v. 24, p. 299–317.

Love, K.M. & Chafetz, H.S., 1988, Diagenesis of laminated travertine crusts, Arbuckle Mountains, Oklahoma: Journal of Sedimentary Petrology, v. 58, p. 441–445.

Merz, M.U., 1992, The biology of carbonate precipitation by cyanobacteria: Facies, v. 26, p. 81–101.

Mylroie, J.E. & Carew, J.L., 1990, The flank margin model for dissolution cave development in carbonate platforms: Earth Surface Processes and Landforms, v. 15, p. 413–424.

Mylroie, J.E. & Carew, J.L., 1995, Geology and karst geomorphology of San Salvador Island, Bahamas: Carbonates and Evaporites, v. 10, p. 193–206.

Northup, D.E., Dahm, C.N., Melim, L.A., Spilde, M.N., Crossey, L.J., Lavoie, K.H., Mallory, L.M., Boston, P.J., Cunningham, K.I. & Barns, S.M., 2000, Evidence for geomicrobiological interactions in Guadalupe caves: Journal of Cave and Karst Studies, v. 6, p. 80–90.

Pavlovic, G., Zupanic, G., Prohic, E. & Tibljaš, D., 2002, Impressions of the biota associated with waterfalls and cascades: Geologia Croatica, v. 55, p. 25–37.

Pedley, H.M., 1987, The Flandrian (Quaternary) Caerwys Tufa, North Wales; an ancient barrage tufa deposit: Proceedings of the Yorkshire Geological Society, v. 46, p. 141–152.

Pedley, H.M., 1994, Prokaryote-microphyte biofilms and tufas: a sedimentological perspective: Kaupia (Darmstadler Beitr. Naturgesch.), v. 4, p. 45–60.

Pedley, H.M., Andrews, J., Ordonez, S., Garcia del Cura, M.A., Gonzales Martin, J.A. & Taylor, D., 1996, Does climate control the morphological fabrics of freshwater carbonates? A comparative study of Holocene barrage tufas from Spain and Britain: Palaeogeography, Palaeoclimatology, Palaeoecology, v. 121, p. 239–257.

Pentecost, A., 1996, Moss growth and travertine deposition: the significance of photosynthesis, evaporation and degassing of carbon dioxide: Journal of Bryology, v. 19, p. 229–234.

Pentecost, A. & Riding, R., 1986, Calcification in Cyanobacteria, *in* Leadbeater, B.S.C. & Riding, R., eds., Biomineralization in Lower Plants and Animals: Oxford, Clarendon Press, p. 73–86.

Pentecost, A. & Zhaohui, Z., 2001, The distribution of plants in Scoska Cave, North Yorkshire, and their relationship to light intensity: International Journal of Speleology, v. 30A, p. 27–37.

Piearce, T., 1975, Observations on the fauna and flora of Ingleborough Cavern, Yorkshire: Transactions of the British Cave Research Association, v. 2, p. 107–115.

Railsback, L.B., Brook, G.A., Chen, J., Kalin, R. & Fleisher, C.J., 1994, Environmental controls on the petrology of a Late Holocene speleothem from Botswana with annual layers of aragonite and calcite: Journal of Sedimentary Research, v. A64, p. 147–155.

Sarigabutr, D., Thummanond, M., Iempairote, T. & Baimoung, S., 1982, Climate in southern Thailand, in Proceedings of the Rattanakosin Bicentennial Joint Seminar on Science and Mangrove Resources: Phuket, Thailand, National Research Council of Thailand and Japan Society for the Promotion of Science, p. 36–46.

Schneider, J. & Le Campion Alsumard, T., 1999, Construction and destruction of carbonates by marine and freshwater cyanobacteria: European Journal of Phycology, v. 34, p. 417–426.

Sevenair, J.P., 1985, The deflected stalactites of Dan-Yr-Ogaf: A hypothesis: NSS Bulletin, v. 47, p. 29–31.

Sweeting, M.M., 1973, Karst Landforms: New York, NY, Columbia University Press, 362 p.

Taboroši, D., 2002, Biokarst on a tropical carbonate island: Guam, Mariana Islands: Theoretical and Applied Karstology, v. 15, p. 73–91.

Taboroši, D. & Hirakawa, K., 2003, Microclimate controls of vadose carbonate precipitation: Evidence from stalactite morphology: Theoretical and Applied Karstology, v. 16, p. 25–40.

Taboroši, D. & Hirakawa, K., 2004, Biota and biologic processes associated with subaerial tufa stalactites in the tropics: Cave and Karst Science, v. 31, in press.

Taboroši, D., Hirakawa, K. & Stafford, K.W., 2003a, Speleothem-like calcite and aragonite deposits on a tropical carbonate coast: Cave and Karst Science, v. 30, p. 23–32.

Taboroši, D., Stafford, K.W., Mylroie, J.E. & Hirakawa, K. 2003b. Littoral dripstone and flowstone: Speleothem-like precipitates on a tropical carbonate coast, Tinian and Rota, Mariana Islands: GSA Abstracts and Programs, v. 35, p. 452.

Taboroši, D., Hirakawa, K. & Stafford, K.W., 2004a, Subaerial tufa in the Mariana Islands and its depositional settings: Studies in Speleology, v. 13, p. 27–41.

Taboroši, D., Hirakawa, K. & Stafford, K., 2004b, Interactions of plant roots and speleothems: Journal of Subterranean Biology, v. 2, p. 43–51.

Thrailkill, J., 1976, Speleothems, *in* Walter, M.R., ed., Stromatolites: Amsterdam, Elsevier, p. 73–86.

Viles, H.A., 1988, Organisms and karst geomorphology, *in* Viles, H.A., ed., Biogeomorphology: New York, NY, Basil Blackwell, p. 319–350.

Viles, H.A. & Goudie, A.S., 1990, Tufas, travertines and allied carbonate deposits: Progress in Physical Geography, v. 14, p. 19–41.

Wasseman, B., 1984, Tiger Cave Monastery: Sawasdee, v. 13, p. 32–38.

Waterhouse, J.B., 1981, Age of the Ratburi Limestone of southern Thailand (the Permian stratigraphy and paleontology of southern Thailand): Bangkok, Thailand, Geological Survey Division, Department of Mineral Resources.

Wefer, F.L., 1991, An annotated bibliography of cave meteorology: Cave Geol., v. 2, p. 84–119.

Weijermars, R., Mulder-Blanken, C.W. & Wiegers, J., 1986, Growth rate observation from the moss-built Checa travertine terrace, central Spain: Geological Magazine, v. 123, p. 279–286.

Wilford, G.E. & Wall, J.R.D., 1964, Karst topography in Sarawak: Journal of Tropical Geography, v. 18, p. 44–70.

Zhaohui Z. & Pentecost, A., 1999, Bryophyte communities associated with travertine formation at Yorkshire National Park, UK: Carsologia Sinica, v. 18, p. 366–374.